

**USE OF DIFFERENT GOLD AMALGAMATION
TECHNIQUES IN MERCURY DETERMINATION
BY COLD VAPOR ATOMIC ABSORPTION
SPECTROMETRY**

**A Thesis Submitted to the
Graduate School of Engineering and Sciences of
İzmir Institute of Technology
in Partial Fulfillment of the Requirements for the Degree of**

MASTER OF SCIENCE

in Chemistry

**by
Arzu ERDEM**

**July 2005
İZMİR**

We approve the thesis of **Arzu ERDEM**

Date of Signature

.....
Assoc. Prof. Dr. Ahmet E. EROĞLU 25.07.2005
Supervisor
Department of Chemistry
İzmir Institute of Technology

.....
Assist. Prof. Dr. Talal SHAHWAN 25.07.2005
Co-Supervisor
Department of Chemistry
İzmir Institute of Technology

.....
Prof. Dr. Emür HENDEN 25.07.2005
Department of Chemistry
Ege University

.....
Prof. Dr. Tamerkan ÖZGEN 25.07.2005
Department of Chemistry
İzmir Institute of Technology

.....
Assist. Prof. Dr. Durmuş ÖZDEMİR 25.07.2005
Department of Chemistry
İzmir Institute of Technology

.....
Assist. Prof. Dr. Şerife YALÇIN 25.07.2005
Department of Chemistry
İzmir Institute of Technology

.....
Assoc. Prof. Dr. Ahmet E. EROĞLU 25.07.2005
Head of Department
İzmir Institute of Technology

.....
Assoc. Prof. Dr. Semahat ÖZDEMİR
Head of the Graduate School

ACKNOWLEDGEMENTS

I would like to express my gratitude to my supervisor Assoc. Prof Dr. Ahmet E. EROĞLU for his excellent supervision, help, guidance and encouragement he provided throughout my thesis. In addition, I am grateful to my co-supervisor Asst. Prof. Dr. Talal SHAHWAN for his valuable comments.

I also would like to thank to members of the thesis committee, Prof. Dr. Emür HENDEN, Prof. Dr. Tamerkan ÖZGEN, Asst. Prof. Dr. Durmuş ÖZDEMİR and Asst. Prof. Dr. Şerife YALÇIN for their valuable comments and patience.

I specially express thanks to Prof. Dr. O. Yavuz ATAMAN, Rsch. Assist. Sezgin Bakırdere and Necati Bey for their help during my study. I am very pleased to Gökhan ERDOĞAN at Material Research Center for his help in performing the SEM/EDS analysis.

I am very grateful to my sister Aslı ERDEM, and my friends Müşerref YERSEL, Murat ERDOĞAN, Filiz PARLAYAN, Demet ERDOĞAN, Özge TUNUSOĞLU and Sinan YILMAZ for their help, patience and encouragement in every step of my study.

Special thanks to Mr. Polat BULANIK for his friendship and support during this thesis.

Finally, I am thankful to my father and mother for their help, love and understanding.

ABSTRACT

A novel amalgamation/cold vapor atomic absorption spectrometric system was developed for the determination of Hg(II) concentration in water samples. In the optimization studies regarding cold vapor atomic absorption spectrometry (CVAAS), effect of concentration and volume of reductant (SnCl_2), carrier gas flow rate and stirring time were investigated and it was found that 500 μl of 5% (m/v) SnCl_2 was optimum for a sample volume of 2.5 ml. The carrier gas flow rate and stirring time were 700 ml min^{-1} and 60 seconds, respectively.

In the next part, an amalgamation unit utilizing various Au-coated sorbents was constructed and tested in the determination of mercury. Among the new amalgamation materials suggested, gold-coated quartz wool was found to be the most efficient although gold sputter-coated carbon fiber gave also very promising results.

Analytical performance of the CVAAS system in terms of sample volume, limit of detection, and without/with amalgamation was also investigated. It was observed that the mercury signal increased with increasing sample volume, as expected. On the other hand, provided that the absolute amount of Hg(II) was kept constant while changing the sample volume, use of amalgamation unit resulted in similar calibration sensitivities. With amalgamation, the linearity and the slope of the calibration plots were not dependant on the sample volume and this property is expected to offer an important advantage since it makes the volume adjustment unnecessary.

The limit of detection was also improved with amalgamation. The highest improvement was obtained with 2.0 ml sample volume; the limit of detection was 3.5 times lower (3.5 times better) than that of without amalgamation when 5-times trapping was employed.

Finally, the analytical performance of the proposed method was tested on a real sample, spring water taken from Karaburun, after spiking with 1.0 $\mu\text{g l}^{-1}$ Hg(II). The results demonstrated that the methodology can be applied to these types of samples directly or after amalgamation, depending on Hg(II) concentration. Other drinking water samples collected from Karaburun were also analyzed using CVAAS (without amalgamation) and none of the samples was found to contain Hg(II) concentration above the limit of detection (0.05 $\mu\text{g l}^{-1}$) for 2.5 ml sample volume.

ÖZET

Sulardaki Hg(II) derişiminin belirlenmesi için yeni bir amalgam oluřturma/soğuk buhar atomik absorpsiyon spektrometri sistemi geliřtirildi. Soğuk buhar atomik absorpsiyon spektrometri (CVAAS) sistemiyle ilgili optimizasyon çalıřmaları sonucunda, 2.5 ml çözeltili hacmi için 500 µl indirgen madde (%5 m/v SnCl₂) hacmi, 700 ml dk⁻¹ taşıyıcı gaz akıř hızı ve 60 s karıřtırma zamanının en uygun kořulları saėladıėı belirlendi.

Sonraki çalıřmalarda, altınla kaplanmış çeřitli adsorban maddelerle bir amalgam oluřturma birimi hazırlandı. Bu maddeler içinde altın kaplı kuvars yün en etkili adsorban olarak belirlendi. Altın aşındırma yöntemiyle hazırlanmış karbon fiberin de etkin bir şekilde kullanılabileceėi gösterildi.

Kullanılan CVAAS sisteminin analitik performansı, çözeltili hacmi, tayin sınırı ve amalgam oluřturma biriminin kullanılıp kullanılmaması açılardan incelendi. Beklendiėi üzere çözeltili hacminin artması cıva sinyalinin de artmasına neden oldu. Diėer taraftan, amalgam oluřturma iřleminin uygulanması halinde, çözeltilerdeki cıva miktarı sabit tutulduğunda, çözeltili hacmi deėiřse bile aynı kalibrasyon duyarlıėı elde edildi. Amalgam oluřturma iřlemi uygulandıėında, kalibrasyon grafiklerinin eėimi ve doėrusallıėında bir deėiřlik olmaması önerilen sistemin avantajıdır; bu sayede analiz sırasında çözeltili hacminin ayarlanmasına gerek kalmayacaktır.

Amalgam oluřturma iřlemi uygulandıėında tayin sınırı da iyileřmiştir. En önemli iyileřme 2.0 ml çözeltili hacmi için elde edilmiştir; 5 kez tutturma gerçekleřtirildiėinde, tayin sınırı 3.5 kat düşmüřtür

Son olarak, önerilen metodun analitik performansı Karaburun (İzmir)'dan alınan ve 1.0 µgl⁻¹ Hg(II) eklenen bir kaynak suyunda denenmiştir. Metodun, Hg(II) derişimine baėlı olarak, numunelere doğrudan ya da amalgam oluřturma iřleminin sonra uygulanabileceėi belirlenmiştir. Karaburun'dan alınan diėer su numuneleri de CVAAS yöntemiyle analiz edilmiş; numunelerin hiçbirinde tayin sınırını (0.05 µgl⁻¹) aşan bir Hg(II) derişimine rastlanmamıştır.

TABLE OF CONTENTS

LIST OF FIGURES	ix
LIST OF TABLES	xi
CHAPTER 1. INTRODUCTION	1
1.1. Introduction to Trace Elements.....	1
1.2. Cold Vapor Atomic Absorption Spectrometry (CVAAS).....	3
1.3. Mercury in Nature.....	5
1.4. Speciation and Determination of Mercury.....	6
1.5. Mercury Amalgamation.....	9
1.6. Characterization of the Solid Surfaces.....	10
1.6.1. Scanning Electron Microscopy (SEM).....	10
1.6.2. Energy-Dispersive X-ray Spectroscopy (EDS/EDX).....	12
1.7. The Aim of this Work.....	12
CHAPTER 2. EXPERIMENTAL.....	13
2.1. Chemicals and Reagents	13
2.2. Instrumentation and Apparatus	14
2.2.1. CVAAS for Hg	14
2.3. Determination of Mercury	16
2.3.1. Optimization of CVAAS Parameters.....	16
2.3.1.1. Effect of SnCl ₂ Concentration	16
2.3.1.2. Effect of SnCl ₂ Volume	16
2.3.1.3. Effect of Carrier Gas Flow-Rate.....	17
2.3.1.4. Effect of Stirring Time.....	17
2.3.1.5. Calibration Plot of Hg(II)	17
2.3.2. Sorption of Hg(II) using Sorbents	17
2.3.3. Desorption from the Sorbents	18
2.4. Mercury Amalgamation.....	19
2.4.1. Preparation of the Amalgamation Materials.....	19
2.4.1.1. Gold-Coated Sorbents.....	19
2.4.1.2. Gold Sputter-Coated Carbon Fibers	19

2.5. Characterization of Solid Surfaces using SEM/EDS	20
2.6. Performance of the Materials Prepared	20
2.6.1. Gold-Coated Alumina and Silica	20
2.6.2. Gold-Coated Quartz Wool	21
2.6.3. Gold Sputter-Coated Carbon Fiber	21
2.6.4. Calibration Plots with and without Amalgamation.....	21
 CHAPTER 3. RESULTS AND DISCUSSION.....	 22
3.1. Determination of Mercury	22
3.1.1. Optimization of CVAAS for Mercury Determinations	22
3.1.1.1. Effect of SnCl ₂ Concentration	22
3.1.1.2. Effect of SnCl ₂ Volume	23
3.1.1.3. Effect of Carrier Gas Flow-Rate	24
3.1.1.4. Effect of Stirring Time.....	24
3.1.1.5. Calibration Plot for Hg(II).....	25
3.2. Sorption of Hg(II) using Solid Sorbents	26
3.3. Desorption from the Sorbents	26
3.4. Performance of the Materials Prepared	27
3.4.1. Gold-Coated Alumina.....	27
3.4.1.1. Trapping/Releasing Temperature	27
3.4.1.2. Calibration Plot for Au-Coated Alumina.....	30
3.4.2. Gold-Coated Silica.....	31
3.4.2.1. Trapping/Releasing Temperature	31
3.4.2.2. Calibration Plot for Au-Coated Silica.....	31
3.4.3. Gold-Coated Quartz Wool	34
3.4.3.1. Trapping/Releasing Temperature	34
3.4.3.2. Calibration Plot for Au-Coated Quartz Wool	36
3.4.4. Gold Sputter-Coated Carbon Fiber	38
3.4.4.1. Trapping/Releasing Temperature	38
3.4.4.2. Calibration Plot for Au Sputter-Coated Carbon Fiber	38
3.5. Analytical Performance of the CVAAS System without and with Amalgamation	40
3.5.1. Effect of Sample Volume on Calibration Sensitivity	40
3.5.2. Effect of Sample Volume on Amalgamation.....	41

3.5.3. Application of the Proposed Method to a Real Sample.....	44
CHAPTER 4. CONCLUSIONS	46
REFERENCES	48

LIST OF FIGURES

<u>Figure</u>	<u>Page</u>
Figure 1.1. The biogeochemical cycling of elemental mercury	5
Figure 1.2. Batch mercury cold vapor generator with drying agent and gold amalgamation preconcentration	10
Figure 2.1. Cold Vapor Atomic Absorption Spectrometry (CVAAS) system and the gold amalgamation unit used in Hg determinations.	15
Figure 3.1. Effect of SnCl ₂ concentration on Hg(II) signal	23
Figure 3.2. Effect of SnCl ₂ volume on Hg(II) signal	23
Figure 3.3. Effect of carrier gas flow rate on Hg(II) signal	24
Figure 3.4. Effect of stirring time on Hg(II) signal.	25
Figure 3.5. Calibration curve of Hg(II).....	25
Figure 3.6. SEM back-scattered microimages of alumina pellets treated with different concentrations of gold solutions.	28
Figure 3.7. Effect of releasing temperature on Hg signal for alumina	29
Figure 3.8. Calibration plot with and without amalgamation for alumina	30
Figure 3.9. SEM back-scattered microimages of silica pellets treated with different concentrations of gold solutions.	32
Figure 3.10. Effect of releasing temperature on Hg signal for silica.....	33
Figure 3.11. Calibration plot with and without amalgamation for silica.....	33
Figure 3.12. SEM back-scattered microimages of quartz wool treated with different concentrations of gold solutions	35
Figure 3.13. Effect of releasing temperature on Hg signal for quartz wool	35
Figure 3.14. Calibration plot with and without amalgamation for quartz wool	36
Figure 3.15. Typical transient signals obtained (a) without and (b) with amalgamation step.....	37
Figure 3.16. SEM back-scattered microimages of carbon fibers sputtered with gold....	38
Figure 3.17. Calibration plot with and without amalgamation for carbon fiber.....	39
Figure 3.18. Calibration plots for different sample volumes without amalgamation as a function of Hg(II) concentration	40
Figure 3.19. Calibration plots for different sample volumes without amalgamation as a function of absolute mass.....	41

Figure 3.20. Calibration plots for different sample volumes with amalgamation as a function of absolute mass.....	42
Figure 3.21. Typical transient signals obtained without and with amalgamation step (five times) when 2.0 ml of 0.2 $\mu\text{g l}^{-1}$ Hg(II) was applied	42
Figure 3.22. Typical transient signals obtained without and with amalgamation step (five times) when 5.0 ml of 0.1 $\mu\text{g l}^{-1}$ Hg(II) was applied	43
Figure 3.23. Typical transient signals obtained without, trapped once and trapped five times with amalgamation step when 10.0 ml of 0.1 $\mu\text{g l}^{-1}$ Hg(II) was applied.....	43
Figure 3.24. The effect of sample volume on trapping/releasing efficiency with and without amalgamation for gold-coated quartz wool	45

LIST OF TABLES

<u>Table</u>	<u>Page</u>
Table 2.1. Properties of the sorbents investigated in this study.....	18
Table 3.1. Sorption of Hg(II) with selected sorbents.....	26
Table 3.2. Elution of sorbed Hg(II) from the sorbents	27
Table 3.3. Efficiency of the Au-coated quartz wool in consecutive traps	37
Table 3.4. Efficiency of the Au sputter-coated carbon fiber in consecutive traps.....	39
Table 3.5. Limit of detection values for different sample volumes without and with five times-trap amalgamation	44

CHAPTER 1

INTRODUCTION

1.1. Introduction to Trace Elements

Increasing concern about the effects of trace elements in various environmental industrial, biological samples necessitate their determination. Trace elements relate to the very small amounts of the analyte found in the sample which requires special instrumental techniques to be determined. Not long ago, trace levels were around mg/kg levels, nowadays concentration levels are ranging from $\mu\text{g/g}$ to ng/g (or even lower). On the other hand, one element at a high concentration in a sample can be considered as a trace in another.

Both natural and anthropogenic activities may change the concentration of trace elements in the environment. Human activities include mining and ore processing, coal and fuel combustion, industrial processing (chemical, metal, alloys or petroleum), agricultural (fertilizers, pesticides and herbicides) and domestic effluents. Weathering of rocks, volcanoes, thermal springs and lake or river sediments are the natural factors that may affect trace elements. The trace element contaminants which enter the environment can have significantly different bioavailability and toxicity in biological processes. Especially, bio-transformation by bacteria in the water-sediment interface can strongly influence elemental toxicity throughout the remaining food chain. For example, Hg, As, Sn and Pb undergo biomethylation in the water-sediment interface, resulting in the production of more toxic species which are concentrated in shellfish and fish. Therefore, trace element analysis is very important for the evaluation of environmental factors (Fifield and Haines 1995).

Trace analysis, or analysis in general, can be considered to include several steps. These are sample collection (if the analysis is not being carried out *in situ*), storage and transportation of the sample to the laboratory, preparation for the measurement, calibration of the instrument (if an instrumental determination is necessary), measurement, data analysis and reporting (Truitt and Weber 1979).

One of the main problems in the sample preparation is the contamination of the sample during sampling, storage and analysis. Therefore, several precautions should be taken in order to prevent contamination. Water samples can be acidified to $\text{pH} < 2$ at time of collection, in order to reduce adsorption of the analytes onto the walls of containers. In addition to this, it is suggested to use all containers for only trace analysis where the reagents of use should be at highest purity. Finally, all steps should be carried out in clean rooms in order to avoid contamination (Welz and Sperling 1999).

Depending on the sensitivity required in the quantitation step, generally two approaches are followed in trace element determinations. The first strategy is to use or develop special measurement systems which are capable of detecting the low concentrations of certain species directly in the sample. Instrumental developments have produced an increasing number of methods suitable for trace element determinations without an enrichment step. For example, atomic absorption spectrometry (AAS), inductively coupled plasma atomic emission spectrometry (ICP-AES) and in recent years inductively coupled plasma mass spectrometry (ICP-MS) have been extensively used in the determination of trace metals in the samples either directly or after a matrix separation step.

The second strategy in trace analysis is to use some preconcentration methods to increase the concentrations of the analytes to a measurable level using available techniques. The chemical techniques used in preconcentration may provide analyte separation from the matrix as well as its preconcentration. Minimization of matrix effects may lead to lower detection limits.

Liquid-liquid extraction (LLE) and solid phase extraction (SPE) are listed among the important preconcentration techniques for metal ions. Liquid-liquid extraction requires the use of large volumes of high purity solvent, so it offers limited preconcentration factors. However, solid phase extraction enables the preconcentration of trace elements and removal of interferences and it also reduces the usage of organic solvents that are often toxic and may cause contamination. Upon elution of the retained compounds by a volume smaller than the sample volume, the concentration of the analyte can be increased before the final determination step. Preconcentration using solid phase extraction can be performed in two ways, the batch and the column method. In the batch mode, a quantity of sorbent and the sample are mixed and the mixture is shaken for a specified time. Then, the sorbent and the solution are separated by filtration where the analyte of interest may become bound to the sorbent. In the column mode, the

sorbent is packed into a suitable column (e.g. a Pasteur pipette, a disposable column, or a microcolumn) through which a known amount of the sample solution is passed. The column preconcentration can be performed in two ways; on-line and off-line. In the former, the sorbent column is coupled directly to the available instrument where sample enrichment, desorption and determination can be carried out simultaneously. In the latter, the sample is passed through the column following its desorption with an eluent in which the final solution is analyzed by an appropriate method. On-line procedures avoid sample treatment between preconcentration and analysis steps, so that analyte losses and risk of contamination are minimized, allowing higher reproducibility. In addition, all the sample volume is further analyzed, which enables smaller sample volumes to be used. In the presence of high matrices, the off-line methods can be preferred due to their flexibility, and the opportunity to analyze the same sample using various techniques. Other useful preconcentration methods are co-precipitation and volatilization (Camel 2003).

1.2. Cold Vapor Atomic Absorption Spectrometry (CVAAS)

The chemical properties of some elements are such that special methods can be used both to separate them from the sample matrix before their introduction into the atomization/ionization unit and to convert them into an atomic vapor. Mercury and those elements which form stable volatile covalent hydrides (As, Bi, Ge, Pb, Se, Sb, Sn, and Te) may be separated from the sample matrix by *vapor generation*.

Mercury is the only metallic element that has a vapor pressure as high as 0.0016 mbar at 20 °C, which corresponds to a concentration of approximately 14 mg/m³ of mercury in the vapor phase. Thus, it is possible to determine mercury directly by AAS without the use of an atomizer. The element must only be reduced to the metallic form and transferred to the vapor phase. This procedure is termed the *cold vapor technique* (Welz and Sperling 1999). The determination of mercury by cold vapor atomic absorption was first proposed by Poluektov and Vitkun in 1963. Four main methods have been used to bring mercury into the vapor phase:

i) Reduction-aeration: This is by far the most common method which is used to bring mercury into the vapor phase. Mercury in aqueous solution is treated with a reducing agent and then swept out of solution by passing a gas through it.

ii) Heating: The sample is pyrolysed and combusted.

iii) Electrolytic amalgamation: Mercury is plated onto a copper cathode during electrolysis and this cathode is then heated in order to release mercury.

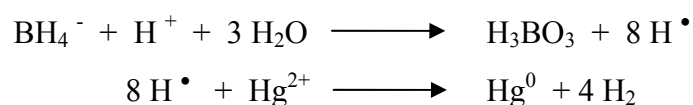
iv) Direct amalgamation: Mercury is collected on a silver or gold wire, from which it is released by heating.

The evolved mercury vapor is passed through an absorption cell, usually constructed of borosilicate glass with silica-end-windows. A transient absorption peak is observed (Ebdon et al. 1998). There are two primary advantages of the cold vapor process. First, mercury is removed from the sample matrix, which reduces the potential for matrix interferences. Second, the detection limits are improved since the entire mercury sample is introduced into the atomizer within a few seconds.

Two reducing agents are exclusively used for cold vapor analysis, tin(II) chloride and sodium borohydride. Tin(II) chloride, SnCl₂, needs the metallic mercury to be transported by an inert gas stream (argon or nitrogen) purged through the solution to drive out the mercury to the absorption cell.



Nevertheless, sodium borohydride in an alkaline solution is becoming the preferred reagent; it requires no other reagents for reduction. Sodium borohydride is a stronger reducing agent than tin(II) chloride. In addition, the sodium borohydride produces hydrogen (H₂) as part of the reduction chemical reaction. (Anderson 2000).



The 253.7 nm line is usually used in mercury determination by AAS, but the transition is spin forbidden, and relatively insensitive. The 184.9 nm line is potentially 20-40 times more sensitive, but at this wavelength most flame atmosphere gases absorb strongly. Thus, flame methods for mercury are not suggested for their sensitivity (Ebdon et al. 1998). Although mercury can be successfully determined by electrothermal AAS (ETAAS), the detection limit is poor and matrix interferences usually occur because high volatility of mercury restricts the ashing temperature.

1.3. Mercury in Nature

Mercury is a natural element that is found in air, water and soil. Mercury cycles in the environment as a result of natural and anthropogenic activities. It rarely occurs in elemental form in nature and is found mainly in cinnabar ore (HgS) (WEB_1 2004). All of its compounds are volatile at temperatures below 500°C and decompose easily to the free metal due to its high vapor pressure. Mercury is released to the environment from many sources. A schematic form of the global mercury cycle is presented in Figure 1.1. As indicated in this figure, mercury is emitted to the atmosphere by a variety of sources, dispersed and transported in the air, deposited to the earth, and stored in or transferred between the land, water, and air (Keating et al. 1997).

Mercury is widely used because of its diverse properties. In very small quantities, mercury conducts electricity, responds to temperature and pressure changes and forms alloys with almost all other metals. Mercury serves an important role as a process or product ingredient in several industrial sectors. In the electrical industry, mercury is used in components such as fluorescent lamps, wiring devices and switches (e.g., thermostats) and mercuric oxide batteries. Mercury is also used in navigational devices, instruments that measure temperature and pressure and other related uses. It is a component of dental amalgams used in repairing dental cavities (Keating et al. 1997).

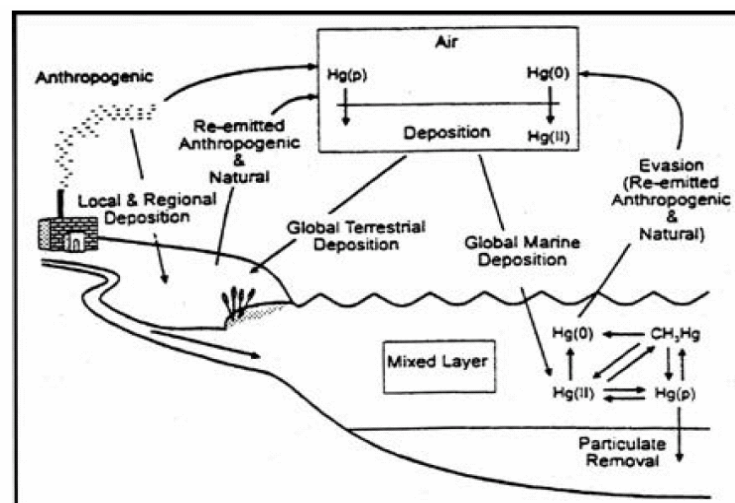


Figure 1.1. The biogeochemical cycling of elemental mercury.
(Source: Keating et al. 1997)

Mercury can exist in three oxidation states: Hg^0 (metallic), Hg_2^{2+} (mercurous) and Hg^{2+} (mercuric). The properties and behavior of mercury depend on the oxidation state. Most of the mercury in water, soil, sediments, or biota (i.e., all environmental media except the atmosphere) is in the form of inorganic mercury salts and organic forms of mercury. Mercury and its compounds are considered as pollutants of priority interest by the Environmental Protection Agency of the United States (USEPA). According to USEPA, maximum contamination level goal (MCLG) and maximum contaminant level (MCL), are both $2 \mu\text{g l}^{-1}$ for the drinking water (WEB_2 2005). The European Union established a maximum admissible concentration of mercury in drinking water of $2 \mu\text{g l}^{-1}$. Typical concentrations of dissolved mercury in unpolluted waters are less than $2.8 \mu\text{g l}^{-1}$ (Anderson 2000).

Two different forms of mercury are of human health concern. The first one, elemental mercury is very toxic in its vapor form. It vaporizes slowly at room temperature or quickly when heated. The other form is organic mercury which can be transformed from elemental and inorganic mercury salts by bacteria. Unlike elemental mercury, organic mercury can be readily absorbed in humans and the most likely source of organic mercury is contaminated fish. Its exposure can result in long term damage to the kidney, liver and central nervous system (Keating et al. 1997).

1.4. Speciation and Determination of Mercury

Many elements and substances exist in water in a variety of physico-chemical forms. These different forms often exhibit different physical, chemical and biochemical properties necessitating the determination of the all species for the analyte of interest. In order to obtain full structural information on the chemical form of the element, the speciation analysis, describing as a measurement which gives qualitative and/or quantitative information on the chemical form of the element, has been developed (Welz 1998). Speciation analysis of environmental samples has become increasingly important, once the behavior of an element is dependent on its distribution among different forms. Thus, speciation analysis assists in understanding its biogeochemical cycling and the identification of the environmental compartments where transformations can take place (Monteiro et al. 2002). For instance, HgS , is an insoluble species, which may deposit in the sediments of a lake. On the other hand, Hg^{2+} ion is very soluble and

will stay dissolved in the water. In the case of cadmium, the salinity of the water determines whether the metal is present as Cd^{2+} or CdCl_4^{2-} where adsorption onto clay particles will change.

Different chemical forms of an element have a variety of effects on the human organisms; for example, these forms may display different reactivity, toxicity, and bioavailability causing a real health risk on people. For this reason, investigation of methods for speciation of trace elements has been of interest for several years.

In natural water speciation studies, a rapid and reliable separation technique coupled with a suitable detection system is required. The samples should be analyzed as soon as possible after collection without use of sample preservation techniques such as acidification which may modify the natural equilibria of species present.

The need for mercury speciation analysis instead of total concentration analysis results from the viewpoints of bioavailability, toxicity, physicochemical behavior and understanding of environmental mercury cycling. The stability of mercury solutions is a major problem since mercury must be determined in trace and ultratrace ranges where losses and contaminations are frequent. The problem becomes complex when a speciation step is required (Welz and Sperling 1999). Many workers have performed the separation of methyl mercury and mercury(II) and determined their concentrations with a subsequent detection system. Wuilloud et al. (2002) described a procedure for the separation and determination of mercury species based on the flow injection-cold vapor atomic absorption spectrometry (FI-CVAAS). The inorganic mercury species were retained on a column filled with a Dowex 1X-8 resin as the anionic complex formed with Methylthymol Blue (MTB) at pH 6.3 and removed them from the column with 3 M HNO_3 . The selectivity of the MTB reagent in the formation of complexes with mercury species prevented the cationic organomercurial species from being retained on the resin. Monteiro et al. (2002) have performed the sequential selective reduction of mercury(II) and methylmercury using two serial gas-liquid separators, coupled to CVAAS. Pager and Gaspar (2002) have used capillary zone electrophoresis (CZE) to separate mercury compounds. In order to achieve this, different complexing agents having thiol group were formed and separated in fused silica capillary at 25 kV using 25 mM sodium borate buffer (pH=9.3). Bagheri and Ghalami (2001) have determined mercury(II) and methylmercury in river waters by cold vapor atomic fluorescence spectrometry (CVAFS) after preconcentrating with 2-mercaptobenzimidazol loaded on silica gel and eluting with 0.05 M KCN solution and 2.0 M HCl to desorb inorganic and

methyl- mercury species, respectively. Mondal and Das (2003) have synthesized a chelating resin [1,2-bis(o-aminophenylthio)ethane] containing nitrogen and sulphur donor that is very selective for mercury. Methylmercury and mercury(II) were eluted with ethanol and thiourea in 1 M HCl, respectively; then analyzed with cold vapor atomic absorption spectrometry (CVAAS). Sun et al. (1997) have proposed a novel method for *in situ* conversion of inorganic mercury to organic mercury combined with the supercritical fluid extraction of the organic mercury by the supercritical carbon dioxide. Dietz et al. (2001) have used the capillary cold trap as a new sample introduction method and have determined mercury species by MIP-AES.

As mentioned before, the presence of mercury species is of great concern as it is well known that inorganic mercury (Hg^{2+}) is converted into highly toxic methylmercury (MeHg^+) by several organisms. Due to the presence of mercury in environmental samples at low levels, its separation from other interfering elements present and the use of a preconcentration step prior to the determination is usually necessary.

There are many methods for the determination of mercury in various samples including, potentiometry (Abbas and Mostafa 2002), flame (Hinds 1998) and furnace atomic absorption spectrometry (Yang et al. 2002), cold vapor atomic absorption spectrometry (Wurl et al. 2000), inductively coupled plasma atomic emission spectrometry (Wuilloud et al. 2002), fluorimetry (Sandor et al. 1999), X-ray fluorescence (Bennun et al. 1999), and voltammetry (Guo et al. 1999). In addition to above mentioned methods several spectrophotometric methods are also reported for the trace determination of mercury using various reagents such as, p-nitrobenzoxosulfamate (Andac et al. 2003). Since mercury must mainly be determined in the trace range, flame atomic absorption spectrometry is not well-suited because of its low sensitivity. Among the determination methods, CVAAS has received great attention for the determination of mercury because of its simplicity, high sensitivity and relative freedom from interferences. Neto et al. (2000) have developed a flow injection system with a cation resin packed microcolumn for the determination of trace levels of mercury in agroindustrial samples by CVAAS where improved sensitivity and selectivity was achieved. A flow system device for the on-line determination of total mercury in sea water is described by Wurl et al. (2000) where the detection limit was improved by using gold amalgam preconcentration method. A novel flow injection method for the determination of mercury at ng l^{-1} levels was developed by Zachariadis et al. (2003) using on-line solid phase extraction and cold vapor atomic absorption spectrometry.

1.5. Mercury Amalgamation

The development of reliable methods for the determination of mercury at (ultra)trace levels in environmental and biological materials is of particular significance and, as mentioned in previous paragraphs, CVAAS and CVAFS are among the most sensitive methods. To lower the detection limit and to improve the sensitivity further, the combination of on-line noble metal amalgamation preconcentration with such techniques has been developed.

Mercury forms amalgams on several metals (Anderson 2000). With this technique, mercury is reduced to the elemental form, Hg(0), using an appropriate reducing agent (e.g. tin(II) chloride). The mercury vapor is liberated from the solution by passage of a gas, such as air, nitrogen or argon, using a gas-liquid separator, and introduced into the absorption cell of AAS. By this way, mercury may be collected either from large sample volumes or over extended periods or both so it enables higher preconcentration factors to be attained. Anderson (2000) determined mercury in the typical manner in which the mercury vapor was passed through an absorber, for example a gold gauze, where it is retained (Figure 1.2). The mercury subsequently released by rapidly heating the absorber to 600 °C and determined using the proper technique. However, there are two disadvantages with this amalgamation preconcentration technique. First, the efficiency of mercury collection may be impaired by moisture or other gaseous reaction products that poison the surface of the amalgamation medium, necessitating occasional cleaning. Second, during heating of the collector to release the mercury, a gas flow is used to transport the vapor to the absorption cell, which means that the sensitivity is flow-rate limited. Slight changes in the flow-rate between measurements will also impair the reproducibility (Li et al. 2002).

Magalhaes et al. (1997) have described a method for the direct determination of mercury in sediments by atomic absorption spectrometry using a pyrolysis chamber. The released mercury is amalgamated on a gold coated collector where mercury vapor is later measured by AAS after thermal desorption. A flow injection system was coupled to an on-line gold amalgamation preconcentration/separation unit to determine organic and inorganic mercury species (Kopysc et al. (2000)).

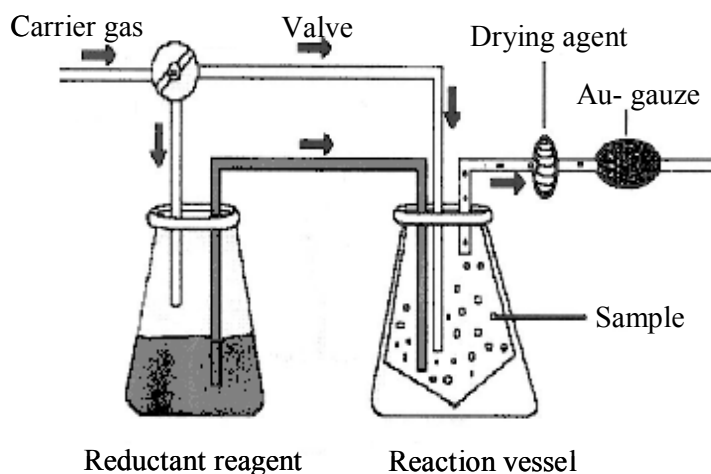


Figure 1.2. Batch mercury cold vapor generator with drying agent and gold amalgamation preconcentration. (Source: Anderson 2000)

A new and rapid technique was proposed by Costley et al. (2000) for the determination of total mercury in environmental and biological samples. This technique features the pyrolysis of the sample in a combustion tube at 750 °C under an oxygen atmosphere, collection on a gold amalgamator and its subsequent detection by AAS. Nakagawa (1999) sampled gaseous mercury in fumaroles by amalgam collectors with gold wire wool. Total dissolved mercury in condense vapor water was separated from stream at atmospheric pressure and then determined by a modified flameless AAS after reduction with tin(II) chloride. Tanida and Hoshino (1990) have developed an aerial mercury continuous monitoring apparatus which combines a mercury collector using a chromosorb P resin coated with gold and determined mercury using flameless atomic absorption.

1.6. Characterization of the Solid Surfaces

1.6.1. Scanning Electron Microscopy (SEM)

Scanning Electron Microscopy is a powerful technique applied in micro-imaging of a variety of surfaces. Although SEM has some disadvantages as limited resolution, damaging polymer surfaces by electron beam, this technique is easy to use and involve easy sample preparation. SEM enables to explore the surface structure to determine particle size and texture on that surface. Prior to SEM analysis, the solid samples are

sprinkled onto adhesive aluminum/carbon tabs supported on metallic disks. Samples are then introduced to the instrument operating under vacuum and microimages, obtained by using electron beams, are recorded. In order to generate demagnified image of electron source lenses are utilized. Specimen is across scanned with this probe of electrons; signals are created as a result of sample-electron interaction. Then, these signals are detected, amplified and utilized to modulate intensity of image tube. The surface of a solid sample is scanned in a raster pattern with a beam of energetic electrons. Several types of signals are produced from a surface in this process, including backscattered, secondary, and Auger electrons; X-ray fluorescence photons; and other photons of various energies. All of these signals have been used for surface studies, but the two most common are backscattered-secondary electrons, which serve as the basis of SEM, and X-ray emission, which is utilized in electron microprobe analysis (Skoog and West 1971). When the sample is bombarded with electrons, many different interactions occur between them. Electrons are reflected from the sample and collected by a detector in which they are converted into a small electrical signal. This signal includes a variety of information about a single point on the surface of sample. In order to obtain an image of the sample a large number of points over an area of sample is needed. The beam is moved point-by-point along a line and the reflected electron signal is collected. A line of 1000 points is completed, then the beam is moved quickly back to the start of that line. The beam is then shifted down one line width and repeats its scan. A complete scan includes 1000 lines in which they are 1000 points (Lawes 1998). There are two main types of sample/electron interactions: unscattered electrons and elastically scattered electrons. Elastically scattered electrons change direction but preserve almost all of their energy with < 1 eV loss. The angle through which the electron is deflected depends on how much energy it has, and how close it passes to the nuclei. Elastic scattering is more likely to be seen in samples of high atomic number, and with low accelerating voltage beams. Through inelastic scattering incident electrons transfer a large proportion of their kinetic energy to the target atoms. Inelastic scattering is more likely to be seen in the lighter elements and gives useful information about the surface of sample and elemental composition of sample.

SEM is near-surface sensitive technique. The primary electron beam causes ionization of atoms on its path which in turn cause ejection of secondary electrons from the solid surface having 0 - 20 eV and they are attracted to positively charged detector.

Secondary electron images can be acquired about to 100 nm. Primary electron beam has the depth of penetration of 0.5 - 5 μm depending upon the density of the solid.

1.6.2. Energy-Dispersive X-ray Spectroscopy (EDX)

In addition to SEM, EDS is a complementary technique that can be applied in the identification of elemental composition of surfaces. This technique has enabled X-rays to be emitted by elements within the surface that are initially excited by bombarding electrons. X-rays are produced by the incident probe in a volume which is similar with these of backscattered electrons and consequently, the elements in a sample within that volume can be recognized by comparing the peaks with the characteristic energies of the elements. Internal corrections for the cross sections of different elements is automatically performed, thus the concentrations of the elements can be calculated.

The dimension of the interaction volume depends on the mean atomic number and the density of the material, the beam energy, and the emitted X-ray energy. The sampling depth in EDS is approximately 1 μm and diameters are ranging from 0.03 μm to several μm . Hence, conventional EDS will not reveal compositional changes owing to surface separation. It is possible, however, by analyzing a point at several different beam energies, to determine the thickness and composition of this surface layers. Moreover, in addition to spot analysis that allows the detection of various elements present in a certain point on the surface of a sample, the distribution of various elements across sections on the surface can also be mapped using EDX mapping analysis. The resulting map, which consists of bright points, shows the location of a particular element and brightness of the points gives information about the concentration of that element.

1.7. The Aim of this Work

The purpose of this work is to develop a novel method for the determination of trace mercury in environmental samples using different gold amalgamation techniques by cold vapor atomic absorption spectrometry. For this reason, several gold coating processes were tried and characterization by scanning electron microscopy and energy-dispersive X-ray spectroscopy were performed.

CHAPTER 2

EXPERIMENTAL

2.1. Chemicals and Reagents

All reagents were of analytical grade. Ultra pure water (18M Ω) was used throughout the study. Glass and plastic ware were cleaned by soaking in 10% (v/v) nitric acid and rinsed with distilled water prior to use.

1. Standard Hg(II) stock solution (100 mg l⁻¹): Prepared by dissolving 0.0338 g of mercury(II) chloride (HgCl₂) (Carlo Erba, Italy) in 250 ml ultra pure water and acidified with 0.14 M HNO₃ (Merck, Germany).
2. Calibration standards: Lower concentration standards were prepared daily from mercury stock standard solution.
3. Tin(II) chloride solution (5% m/v): Prepared daily from its stock solution (SnCl₂.2H₂O) (Merck, Germany) in 0.96 M HCl (Merck, Germany) (v/v) for the reasons of solubility and stability.
4. Auric acid solution: Prepared daily by dissolving appropriate amount of auric acid (HAuCl₄.3H₂O) (Sigma, Germany) in aqua regia (1:3 HNO₃/HCl).
5. Gold solution: Prepared by dissolving metallic gold (92 % purity; bought from the jewelry shop) in aqua regia (1:3 HNO₃/HCl) on a hot plate for one hour.

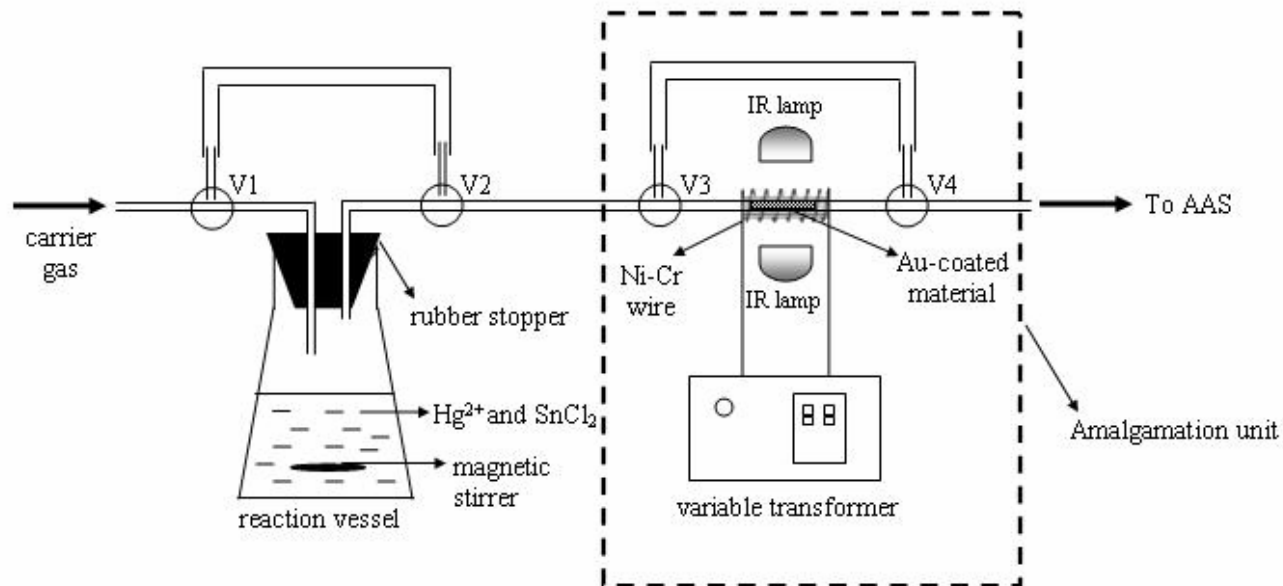
2.2. Instrumentation and Apparatus

An atomic absorption spectrometer, Thermo Elemental Solaar M6 Series was used for the measurements. Mercury determinations were performed with CVAAS. In sorption studies with batch process, Yellowline RS 10 orbital shaker (Staufen, Germany) was used to provide efficient mixing. The manifold for on-line preconcentration system utilized a reaction vessel, a magnetic stirrer to ensure rapid reactions, a transformer station, glass columns, and tygon tubings. A glass absorption cell with quartz windows mounted on the standard air-acetylene burner was used for the determination of mercury by the cold vapor technique (the details of the system are outlined in the following section). The pH measurements were performed by using Corning 450 pH/ion meter with a combination pH electrode.

2.2.1. CVAAS for Hg

For mercury, samples/standards are placed in the 100-ml reaction vessel, 500 μ l of 5% (m/v) SnCl_2 was added with pipette, the vessel is closed, and then the solution is mixed by magnetic stirrer. After a certain reaction/equilibrium time, mercury atoms are formed and then separated from the liquid phase as an atomic vapor. An inert gas (N_2) is passed through the reaction vessel to carry the atomic mercury and into the glass tube having quartz windows aligned in the optical path of AAS. Glass tube atomizer was 15 cm long (8 mm i.d., 10 mm o.d.) and had inlet and outlet tubes at two ends for the introduction and venting of mercury.

The amalgamation unit used two 150 W infrared lamps (General Electric Co. USA) to heat the analytical trap. The thermal desorption unit used for the gold amalgam sample trap was constructed in the laboratory by wrapping a coil of Ni-Cr wire (20 gauge) 30 mm in length, about 5 turns per 10 mm. A 8 A, 220 V AC input and 45 V AC output variable transformer was used to heat the sample trap. In order to decrease the cooling time, the gold column was kept under an argon atmosphere continuously. In addition to argon gas, two small fans were used to cool the amalgamation unit to room temperature. Temperature measurements were made with a Ni-Cr thermocouple with a ceramic coated tip. A transient atomic absorption peak was obtained. CVAAS and the gold amalgamation systems used in mercury determinations are shown in Figure 2.1.



Function	Positions of the 3-way valve			
	V1	V2	V3	V4
Carrier gas flow between measurement cycles	⊕	⊕	⊕	⊕
Cold vapor Hg generation (no amalgamation)	⊕	⊕	⊕	⊕
Cold vapor Hg generation followed by amalgamation	⊕	⊕	⊕	⊕

Figure 2.1. Cold Vapor Atomic Absorption Spectrometry (CVAAS) system and the gold amalgamation unit used in Hg determinations (positions of the 3-way valves, V1, V2, V3 and V4, indicate the flow directions during various steps).

Mercury hollow cathode lamp was operated with a maximum current of 6 mA at 253.6 nm and deuterium (D2) background correction was used in all measurements. The monochromator slit was kept at 0.5 mm.

2.3. Determination of Mercury

2.3.1. Optimization of CVAAS Parameters

In order to obtain sensitive, accurate and reproducible results, the first part of the study was focused on the optimization of CVAAS system. Since the analytical performance of the method is influenced by several factors such as the carrier gas flow-rate, the concentration and the volume of SnCl_2 and stirring time, these parameters were optimized. Peak heights of the transient signals were used in all quantitative determinations.

2.3.1.1. Effect of SnCl_2 Concentration

The first parameter optimized was the concentration of SnCl_2 . Since it is known that the sensitivity of the system is affected by SnCl_2 concentration, it is important to find the optimum concentration of SnCl_2 to obtain the maximum signal. For this purpose, 50 ng of Hg(II) in 2.8 M HNO_3 were analyzed with different concentrations of SnCl_2 solution from 1-20% (m/v) and the absorbance signals were obtained.

2.3.1.2. Effect of SnCl_2 Volume

The influence of SnCl_2 volume was investigated to achieve the optimum signal. 50 ng Hg(II) of was prepared in 2.8 M HNO_3 and analyzed by CVAAS using different volumes of SnCl_2 varying in the range of 100-2000 μl .

2.3.1.3. Effect of Carrier Gas Flow-Rate

The flow-rate of the sample through the atomizer is a very important parameter as it affects peak shape and the time of analysis. So, in order to obtain optimum signal for mercury, the carrier gas flow-rate, used to transport metallic mercury vapor into the atomizer tube was also optimized. For this purpose, 50 ng Hg(II) solution was prepared and analyzed by CVAAS system using different flow-rates from 100 to 700 ml min⁻¹.

2.3.1.4. Effect of Stirring Time

The time of reaction was defined as the time necessary to achieve a stable Hg signal, corresponding to an efficient atomic vapor generation. Stirring time should be the same for all solutions to obtain a complete reaction between mercury in the vapor and liquid phases. Different times were assayed, between 0-150 seconds to measure a Hg standard of 50 ng using the optimum conditions.

2.3.1.5. Calibration Plot for Hg(II)

In order to plot the calibration curve of Hg(II), standard solutions from 1.0 ng to 50.0 ng were prepared in 2.8 M HNO₃ and the absorbance signals were obtained by CVAAS and 5% (m/v) SnCl₂ was used as the reductant.

2.3.2. Sorption of Hg(II) using Sorbents

In order to obtain the appropriate sorbent for Hg(II), various adsorbents such as ion-exchange or chelating resins, natural and synthetic zeolites were investigated. The sorption experiments were performed with the batch method because of the small particle size of most of the materials tested. As an initial experiment, 50 ng solutions of Hg(II) were prepared from its stock solution. The pH of the solutions was adjusted to 7.0 since the pH of the natural waters lies generally between 6.0 and 8.0. To 20.0 ml of this solution, 0.100 ± 0.05 g of the tested sorbent was added and the mixture was shaken

manually for 1-2 minutes before being placed on the shaker for a further 15 minutes at room temperature. At the end of the shaking period, the mixture was filtered and filtrate was analyzed by CVAAS using the optimum conditions for percent sorption. The properties of the sorbents tested are given in Table 2.1.

Table 2.1. Properties of the sorbents investigated in this study.

Type	Sorbent	Functional Groups
Strong cation exchanger	Diaion PK 228	Sodium form
	Diaion SK 116	Sodium form
	Amberlite IR-120 plus	Sodium form
	Rexyn I-300	Hydrogen form
	Dowex 50W X8	Hydrogen form
Chelating resin	Duolite C-467	Sodium form
	Duolite GT-73	Free base
	Muromac	Iminodiacetate groups
Zeolite	Clinoptilolite (natural)	^a
	Mordenite (synthetic)	Ammonium form
	Zeolite Beta (synthetic)	Ammonium form
	Zeolite Y (synthetic)	Ammonium form
	Zeolite ZSM-5 (synthetic)	Ammonium form

^a Approximate chemical composition: $(K, Na, \frac{1}{2} Ca)_2O \cdot Al_2O_3 \cdot 10 SiO_2 \cdot 8 H_2O$

2.3.3. Desorption from the Sorbents

After deposition of Hg(II) on the sorbent (as will be shown later, Duolite GT-73 was used as the sorbent) its release was investigated using several eluents. For this purpose, 0.100 ± 0.05 g of sorbent was added to 10 ml of 100.0 ng Hg(II). After shaking for 15 minutes, the mixture was filtered and the sorbent was taken into the eluent. The new mixture was shaken once again for 15 minutes. At the end of this period, the solution was filtered and the eluate was analyzed for its Hg(II) content using CVAAS.

2.4. Mercury Amalgamation

2.4.1. Preparation of the Amalgamation Materials

Two different strategies were followed to coat the target substances with gold. Alumina, silica and quartz wool coatings were carried out at 560 °C by heating in a muffle furnace while the carbon fibers were coated with sputtering. The details are explained in the following sections.

2.4.1.1. Gold-Coated Sorbents

For the preparation of gold coatings for alumina and silica, 1.0 g of the appropriate sorbent were weighed and transferred into a porcelain crucible containing 1.5 ml of gold solution at various concentrations (0.01 to 0.5% (m/v)). In the preparation of the gold-coated quartz wool, 0.20 g of the material was immersed into 1 ml of 0.5% (m/v) gold solution. The mixtures were first heated to dryness on a hot plate to remove excess acids; then, were placed in a muffle furnace for 2 hours at 560 °C. The gold-coated sorbents were transferred into a desiccator and cooled to room temperature. Blanks for the above mentioned materials were also prepared by treating alumina, silica and quartz wool in aqua regia to compare the surface of the gold-coated and the uncoated materials using Scanning Electron Microscopy.

For the preparation of the traps that will be used in the amalgamation unit, 0.3 cm id quartz tubes were filled with the gold-coated sorbents. Untreated quartz wool was used as stoppers at column ends. In alumina- and silica-based columns, the amount of the wool was kept minimal in order to prevent back pressure.

2.4.1.2. Gold Sputter-Coated Carbon Fibers

Preparation of the gold sputter-coated carbon fibers was performed by sputter-deposition from a gold cathode onto a carbon fiber substrate (Gencoa Magnetron Sputtering Cathode). Sputtering is a vacuum evaporation process which physically removes portions of a coating material called the target. The material to be sputtered,

here the carbon fiber, was mounted in a chamber filled with argon gas at low pressure (10^{-2} torr). Positively charged Ar ions are produced when high voltage is applied to the Au cathode target. As these ions collide with the gold target, gold atoms are ejected and coated onto the carbon fiber substrate.

2.5. Characterization of Solid Surfaces using SEM/EDX

SEM/EDX characterization was performed using a Philips XL-30S FEG type instrument. Prior to analysis, solid samples were sprinkled onto adhesive carbon tapes which were supported on metallic disks. Aluminum tapes were not used, as alumina surfaces were also examined. Images of the sample surfaces were recorded at different magnifications. Energy-dispersive X-ray Spectroscopy (EDX) analysis was carried out on randomly selected points on the solid surfaces and back-scatter electron (BSE) detector was utilized during SEM analysis. The backscatter electron detector allows materials with different compositions to be imaged as different (greyscale/atomic) contrast and it is used for the elements having a large atomic number difference between each other. During the measurements, 15 kV was applied with a 36x magnification.

2.6. Performance of the Materials Prepared

2.6.1. Gold-Coated Alumina and Silica

Different concentrations of gold solutions (0.01 – 0.5% m/v) were prepared in aqua regia and 1.0 g of alumina (63 – 200 μm particle size) or silica (63 – 200 μm particle size) was placed in each solution separately. The usual coating procedure was applied as explained in 2.4.1.1.

The trapping/releasing temperature of the gold-coated alumina or silica was determined by preparing 20 ng Hg(II) in 0.7 M HNO_3 and the mercury vapor was obtained after the addition 5% (m/v) SnCl_2 solution. After the optimum stirring time (60

seconds) the mercury vapor generated was passed through the gold-coated alumina or silica column. The releasing temperature was changed between 50 °C to 900 °C.

2.6.2. Gold-Coated Quartz Wool

Different concentrations of gold solutions (0.1 – 0.5% m/v) was prepared in aqua regia and 0.2 g of quartz wool was placed in each solution separately. The usual coating procedure was applied as explained in 2.4.1.1.

The trapping/releasing temperature of the quartz wool was determined by preparing 20 ng Hg(II) in 0.7 M HNO₃ and the mercury vapor was obtained after the addition 5% (m/v) SnCl₂ solution. After the optimum stirring time (60 seconds) the mercury vapor generated was passed through the gold-coated alumina or silica column. The releasing temperature was changed between 50 °C to 950 °C.

2.6.3. Gold Sputter-Coated Carbon Fiber

Gold sputter-coated carbon fiber was prepared as explained in 2.4.1.2. The trapping/ releasing temperature of the material was determined by preparing 20 ng Hg(II) in 0.7 M HNO₃ and the mercury vapor is obtained after the addition 5% (m/v) SnCl₂ solution. After the optimum stirring time (60 seconds) the mercury vapor generated was passed through the carbon fiber column. The releasing temperature was changed between 400 °C and 900 °C.

2.6.4. Calibration Plots with and without Amalgamation

Absorbance values of aqueous calibration standards (1 to 20 ng Hg(II) in 0.7 M HNO₃) were obtained using CVAAS under optimum conditions, with and without amalgamation.

CHAPTER 3

RESULTS AND DISCUSSION

3.1. Determination of Mercury

3.1.1. Optimization of CVAAS for Mercury Determinations

Many methods have been developed for the determination of mercury in environmental samples and CVAAS is among the most popular techniques due to its simplicity, high sensitivity and relatively low cost. This method is sensitive enough for several environmental applications, although in some cases preconcentration procedures based on amalgamation are required. In this study, the initial stages have focused on the optimization of the CVAAS measurements as a different enrichment procedure and different chemicals were employed. Optimization of carrier gas flow-rate, stirring time, volume and concentration of SnCl_2 were carried out. In the initial studies, 2.5ml sample volume was employed and the optimizations were based on this volume. During amalgamation studies, on the other hand, the effect of different sample volumes (2.0, 5.0, and 10.0 ml) were also investigated to have a better comparison.

3.1.1.1. Effect of SnCl_2 Concentration

The first parameter to be examined was the effect of SnCl_2 concentration on the production of the mercury vapor. Figure 3.1 demonstrates the effect of SnCl_2 concentration on the absorbance signal of Hg(II). Although 20% (m/v) SnCl_2 gave the highest absorbance, the increase over 5% (m/v) SnCl_2 was only very slight. Hence, 5% (m/v) SnCl_2 was used throughout the study as it was very difficult to keep the higher concentration of SnCl_2 in solution. This concentration was also thought to be the optimum in terms of cost-effectiveness.

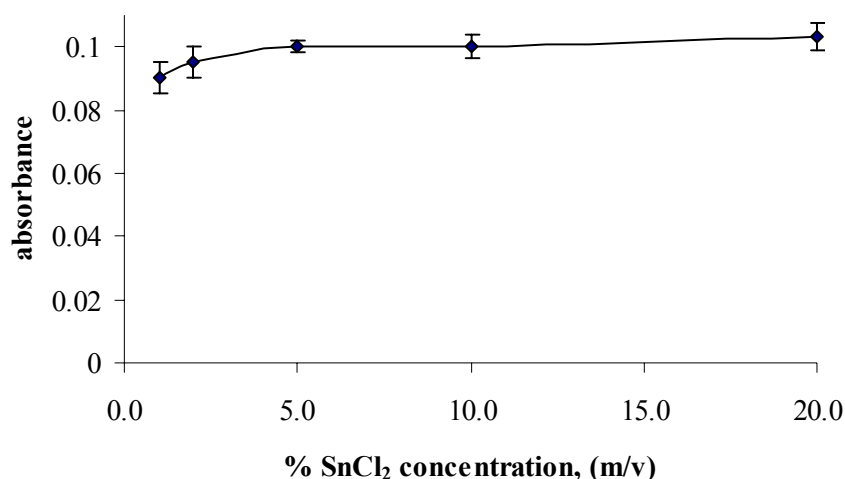


Figure 3.1. Effect of SnCl₂ concentration on Hg(II) signal. (50.0 ng Hg(II))

3.1.1.2. Effect of SnCl₂ Volume

In order to determine SnCl₂ volume on the absorbance signal of Hg(II), various volumes of 5% (m/v) SnCl₂ were added to the solution containing an absolute amount of 50.0 ng Hg(II). 250 μl of SnCl₂ gave the maximum absorbance as shown in Figure 3.2, however, 500 μl of SnCl₂ was chosen as there may be situations where the use of higher amounts of the reducing agent is necessary.

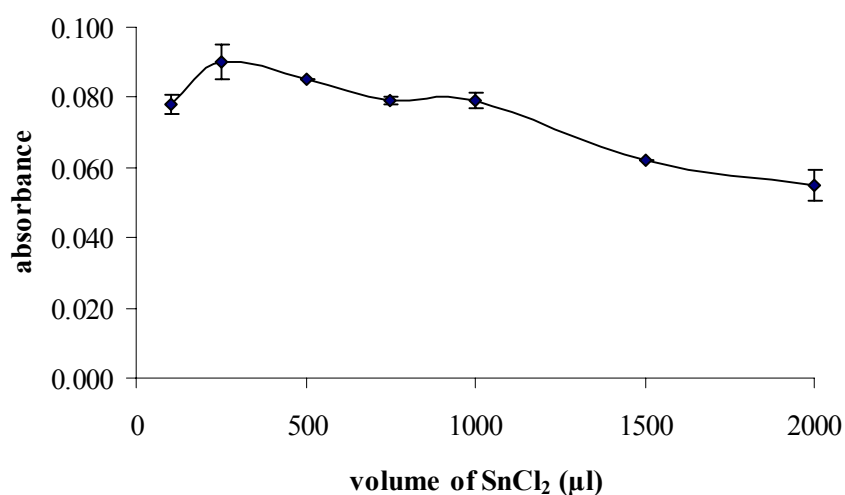


Figure 3.2. Effect of SnCl₂ volume on Hg(II) signal. (50.0 ng Hg(II), 5% SnCl₂)

3.1.1.3. Effect of Carrier Gas Flow-Rate

The carrier gas flow rate is also an important parameter affecting the sensitivity, reproducibility and analytical throughput. Consequently, the carrier gas used to transport atomic mercury vapor was also optimized. In order to achieve this, a solution containing an absolute amount of 50.0 ng Hg(II) was prepared and analyzed using 500 μl of 5% (m/v) SnCl₂ solution at different flow rates varying within 100-700 ml min⁻¹. As seen from Figure 3.3, there is no significant difference at flow rates between 400 and 700 ml min⁻¹. Nevertheless, 700 ml min⁻¹ flow-rate is chosen throughout the study in order to transfer the atomic mercury vapor from the system as quickly as possible.

3.1.1.4. Effect of Stirring Time

The stirring time is necessary to obtain a stable mercury signal, so, equilibration time for the mercury reduction reaction was also investigated. For this purpose, different stirring times were tried, between 0 and 150 seconds. A standard Hg(II) solution containing an absolute amount of 50.0 ng and 500 μl of 5% (m/v) SnCl₂ were used in this study. As seen in Figure 3.4, the absorbance was maximal when the reaction time was between 40 and 60 seconds; therefore 60 seconds was chosen for this study.

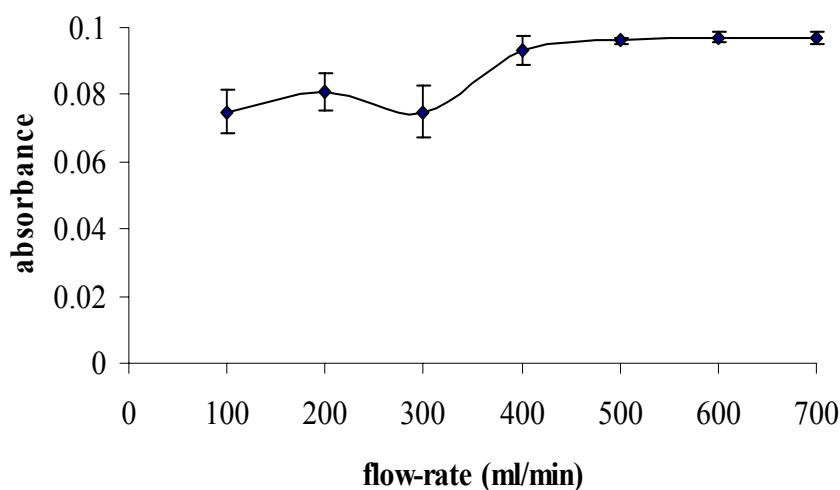


Figure 3.3. Effect of carrier gas flow rate on Hg(II) signal. (50.0 ng Hg(II), 500 μl of 5% (m/v) SnCl₂)

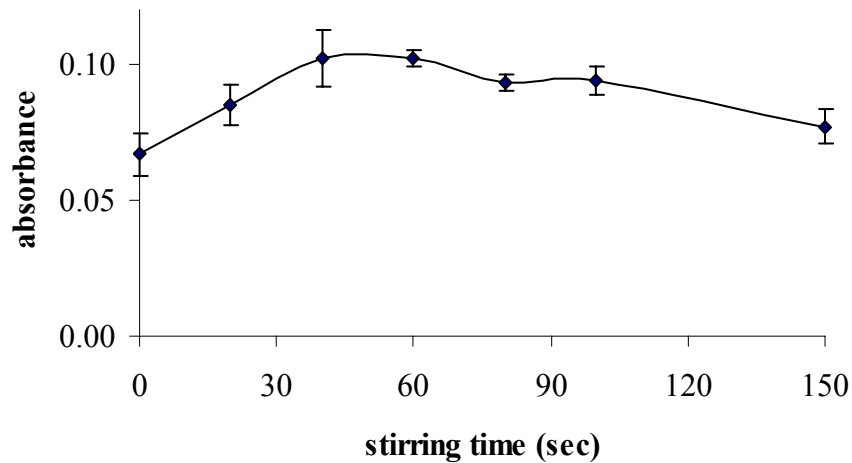


Figure 3.4. Effect of stirring time on Hg(II) signal. (50.0 ng Hg(II), 500 μ L of 5% (m/v) SnCl₂)

3.1.1.5. Calibration Plot for Hg(II)

Absorbance versus concentration plot was obtained for Hg(II) as shown in Figure 3.5. The calibration curve was linear at least up to 400 ng Hg(II). The limit of detection (LOD) based on 3s (3 times the standard deviation above the blank value) was found as 0.35 ng.

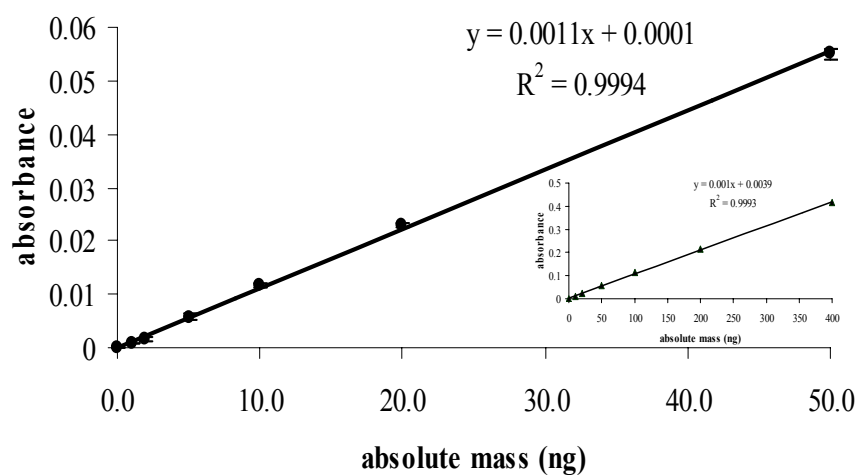


Figure 3.5. Calibration curve of Hg(II), ($y = 0.011x + 0.0001$, $R^2 = 0.9994$), (500 μ l of 5% (m/v) SnCl₂, 2.5 ml sample volume).

3.2. Sorption of Hg(II) using Solid Sorbents

As explained in section 2.3.2, various adsorbents were investigated for Hg(II) sorption using batch process. Table 3.1 gives a rough idea about the uptake of selected sorbents towards Hg(II). As can be seen, there are many candidate sorbents for Hg(II) sorption, but Duolite GT-73, a macroporous resin with a crosslinked polystyrene matrix bearing thiol (–SH) functional groups, offered the most efficient results at pH 7 and the remaining experiments were performed using this resin.

3.3. Desorption from the Sorbents

In order to desorb Hg(II) from the Duolite GT-73 resin, several solutions namely KIO₃, HNO₃, KOH, NH₃, H₂SO₄, HCl and CH₃COOH were prepared and examined. After the usual sorption process, the mixture was filtered through filter paper and the resin was taken into the eluent. The mixture was shaken for another 15 minutes and at the end of this period, the contents were filtered and the filtrate was analyzed by CVAAS. The eluent concentrations and the corresponding recoveries are given in Table 3.2.

Table 3.1. Sorption of Hg(II) with selected sorbents (initial study). (50.0 ng Hg(II), sample volume = 20 ml, amount of sorbent = 0.100 g, pH = 7)

Sorbents	% Hg(II) Sorption
Diaion PK 228	> 85
Diaion SK 116	> 80
Amberlite IR-120	~ 90
Rexyn I-300	~ 90
Dowex 50W X8	> 30
Duolite C-467	~ 90
Duolite GT-73	> 95
Muromac	> 40
Clinoptilolite	> 60
Mordenite	> 85
Zeolite Beta	> 80
Zeolite Y	> 70
Zeolite ZMS-5	> 60

Table 3.2. Elution of sorbed Hg(II) from the sorbents. (100.0 ng Hg(II), sample volume = 20 ml, amount of sorbent = 0.100 g, pH = 7)

Eluent	% Desorption
0.05 M KIO ₃ in 2 M HCl	< 5
2 M KOH	< 5
2 M NH ₃	< 5
2 M H ₂ SO ₄	< 5
4 M HCl	~ 15
4 M HCl (50 °C)	~ 50
2 M CH ₃ COOH	< 5
3 M HNO ₃	< 5
3 M HNO ₃ (50 °C)	~ 70
6 M HNO ₃	~ 10

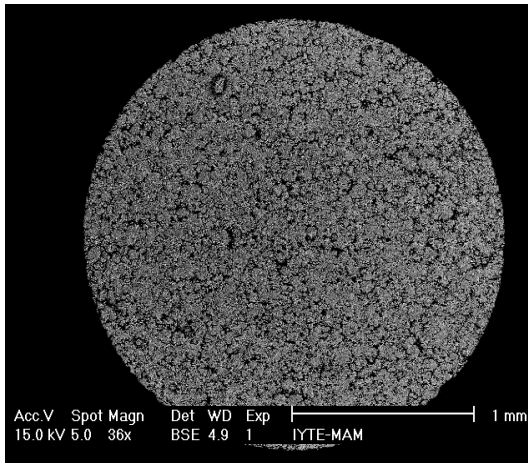
3.4. Performance of the Materials Prepared

3.4.1. Gold-Coated Alumina

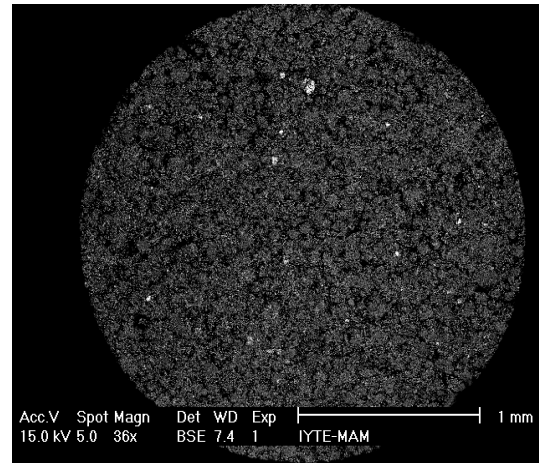
3.4.1.1. Trapping/Releasing Temperature

As explained in section 2.6.1, alumina was treated with different concentrations of gold solutions (0.01 – 0.5% m/v) and the resultant mixture was cured at 560 °C. The SEM back-scattered microimages of the surfaces prepared are shown in Figure 3.6. As seen from the figure, only 0.5 g Au-coated alumina demonstrates an appreciable gold coating on the surface. Still, the sorption behavior of the other surfaces was also investigated in the case where their gold coating was sufficient for the sorption of very small amounts of mercury studied in the present work. In the first part of the study, the trapping temperature was attempted to be optimized and it was found that the material was very efficient in the sorption of atomic Hg vapor even at room temperature (~ 30 °C). Because of this reason, the higher trapping temperatures were not applied.

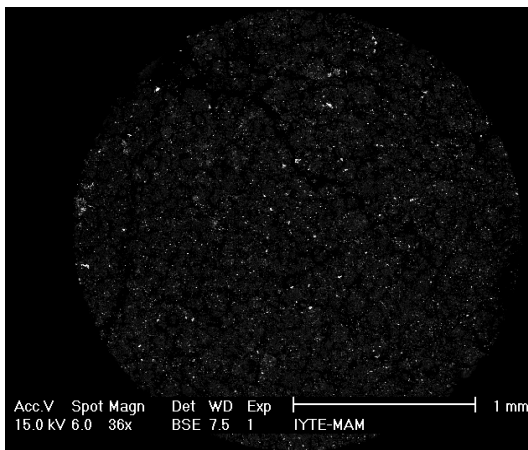
The change in Hg signal as a function of releasing temperature setting for 0.5 g Au-coated alumina is shown in Figure 3.7. Here, it should be mentioned that the actual temperature inside the amalgamation column did not stay constant and continued to increase although the temperature of the Ni-Cr thermocouple reached the pre-set value. The increase was high for lower temperatures (< 400 °C) and was negligible for the



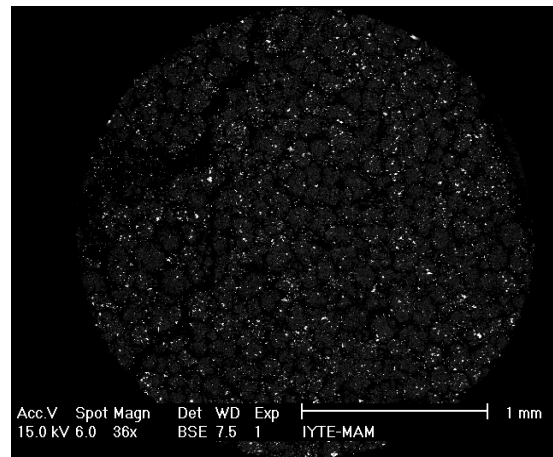
Alumina blank



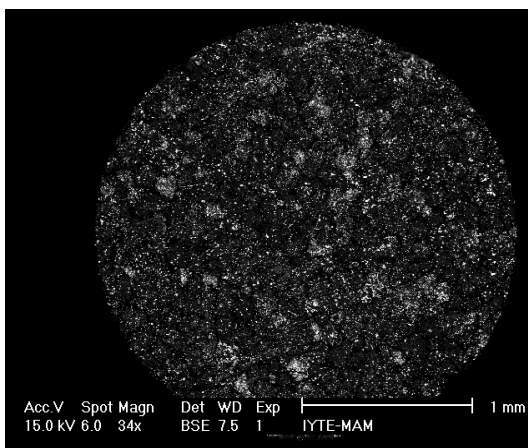
0.01 g Au coated alumina



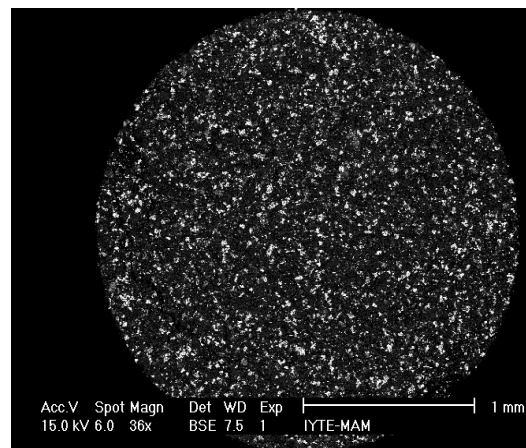
0.05 g Au coated alumina



0.1 g Au coated alumina



0.25 g Au coated alumina



0.5 g Au coated alumina

Figure 3.6. SEM back-scattered microimages of alumina pellets treated with different concentrations of gold solutions.

higher. For example, when the temperature was set to 50 °C, the actual temperature in the column increased to 250 °C whereas it increased only to 930 °C when it was set to 900 °C. This is also the reason for why IR lamps were used during the initial optimization studies for trapping temperature instead of electrical heating.

As seen from Figure 3.7, Hg signal increased with the increase in the releasing temperature (up to 600 °C). At 400 °C, a second peak was observed due to consecutive heating cycles indicating the inefficiency of this temperature to desorb mercury quantitatively (not shown). In addition to this, relatively higher standard deviations were observed for 400 °C. When the temperature was set to 600 °C, it was found that the release from the sorbent was quantitative. At a higher temperature (900 °C), a similar absorbance signal was obtained. As a result, it was decided to use 600 °C as a releasing temperature for alumina for optimum results since there was also no memory effect observed at this temperature.

For the alumina samples treated with different concentrations of Au, similar amalgamation/releasing experiments were carried out and it was found that the less the coated amount of Au on the surface, the less sensitive and the less repeatable the signal. For example, 0.1 g Au-treated alumina demonstrated almost 60% less sensitivity than the optimum. The situation with 0.01 g Au-treated alumina was unacceptable in terms of both sensitivity and repeatability.

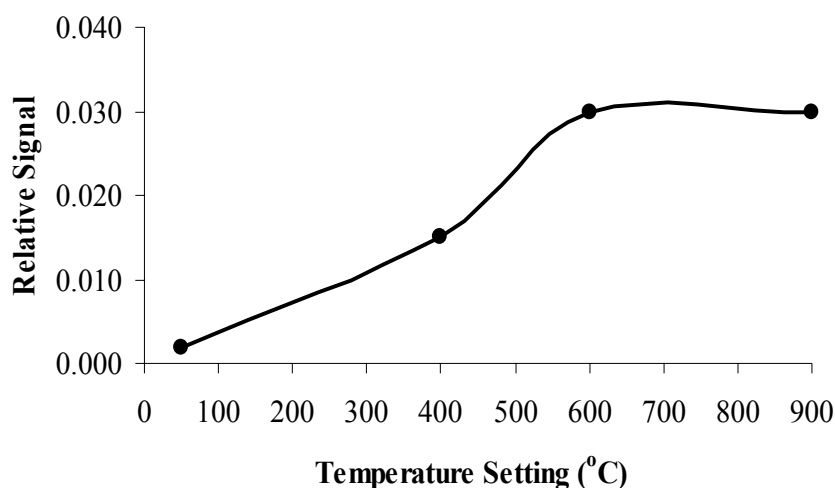


Figure 3.7. Effect of releasing temperature on Hg signal (0.5 g Au-coated alumina, 0.7 M HNO₃, 5% (m/v) SnCl₂).

3.4.1.2. Calibration Plot for Au-Coated Alumina

The calibration graphs of Hg(II) with and without amalgamation with 0.5 g Au-treated alumina are shown in Figure 3.8. Without amalgamation, the Hg vapor was directly sent to the atomizer right after its generation in the reaction vessel and Hg signal was obtained. With amalgamation, on the other hand, the Hg vapor generated in the reaction vessel was passed through the amalgamation column and trapped for 30 seconds. The Hg signal was obtained after the deposited Hg was released from the column with the usual desorption procedure. As can be seen from Figure 3.8, the calibration sensitivity (slope of the calibration plot) is higher with amalgamation. This result could possibly be due to two reasons; firstly, with amalgamation, the Hg deposited is released from a smaller volume (consider the diameter of the amalgamation column) and not diluted to a great extent with the carrier gas on the way to the atomizer tube. Secondly, the kinetic energy of Hg vapor increases upon heating and therefore the vapor zone reaches the atomizer faster than the generated by only CVAAS system.

An interesting observation was obtained with alumina blank (treated only with aqua regia in the same manner). The Hg vapor generated in the reaction vessel was adsorbed by alumina; but it could not be desorbed from the column even at the maximum possible temperature that could be employed in the present system (1000 °C). This observation can show the very strong interaction between the Hg vapor and the alumina surface and can be the topic of further studies with additional experiments.

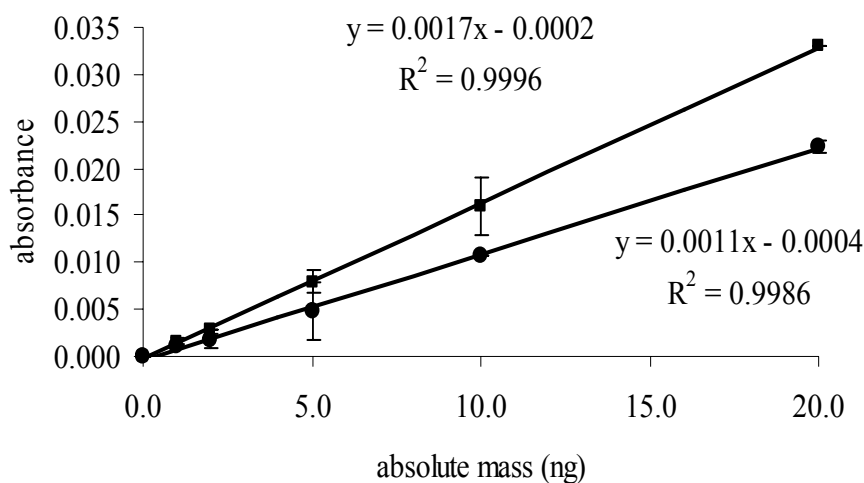


Figure 3.8. Calibration plot with and without amalgamation for alumina. (●)without amalgamation, (■) with amalgamation (0.7 M HNO₃, 5% (m/v) SnCl₂, 2.5 ml sample volume).

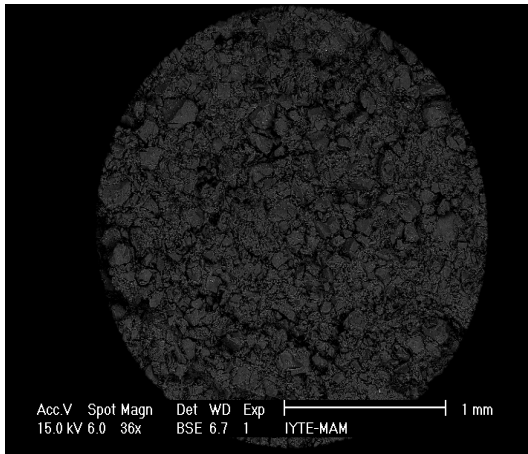
3.4.2. Gold-Coated Silica

3.4.2.1. Trapping/Releasing Temperature

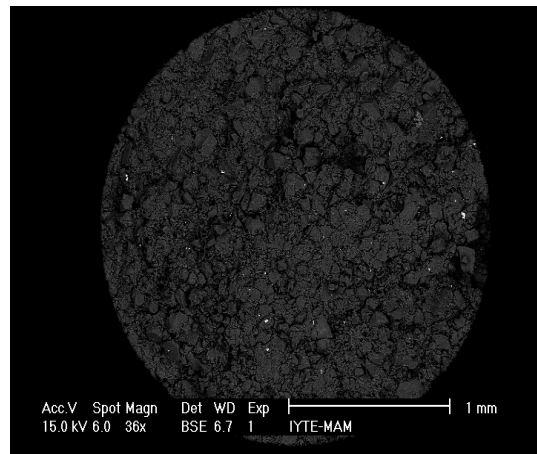
The same procedure followed for alumina was also applied for silica to investigate its analytical performance towards Hg vapor (Section 2.6.1). By using different gold solution concentrations (0.01 – 0.5% (m/v)), silica was handled and cured at 560 °C as in the case of alumina. The SEM back-scattered microimages of the surfaces are shown in Figure 3.9. According to the figure, only 0.5 g Au-coated silica demonstrates an appreciable gold coating on the surface. But, in contrast to alumina, the Au-coating on silica was less uniformly distributed on the surface and a kind of coagulation of gold particles was observed. This inhomogeneous nature of Au-coating was probably the reason for the difficulty in getting reproducible results for silica compared to Au-coated alumina. It should also be mentioned that the small particle size of the silica used in this study was not very suitable for the amalgamation column and caused significant back pressure which does not fit to the purpose of this study. The results of the desorption study are shown in Figure 3.10. The inhomogeneous character of the amalgamation column can also be gathered from the graph and it was necessary to apply a very high temperature to desorb Hg from the column. The blank silica trapped approximately one-fourth of the total Hg generated in the reaction vessel.

3.4.2.2. Calibration Plot for Au-Coated Silica

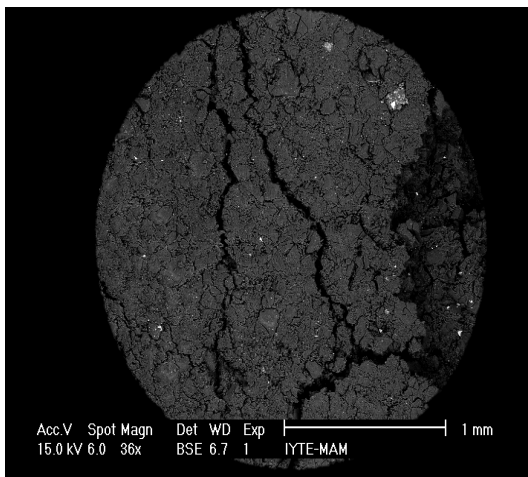
The calibration graphs of Hg(II) with and without amalgamation with 0.5 g Au-treated silica are shown in Figure 3.11. As in the case of alumina, the calibration sensitivity (slope of the calibration plot) is higher with amalgamation since the same principles apply here as well.



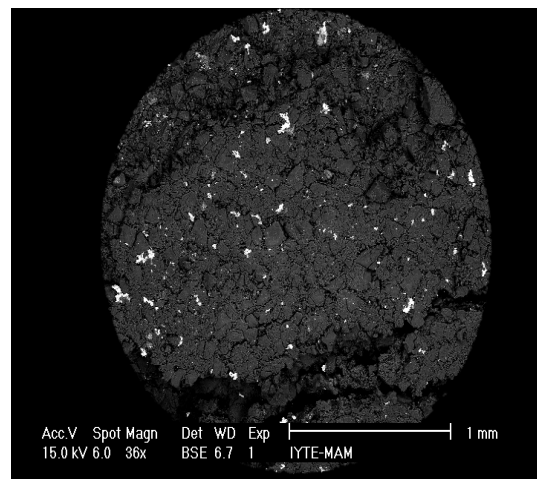
Silica blank



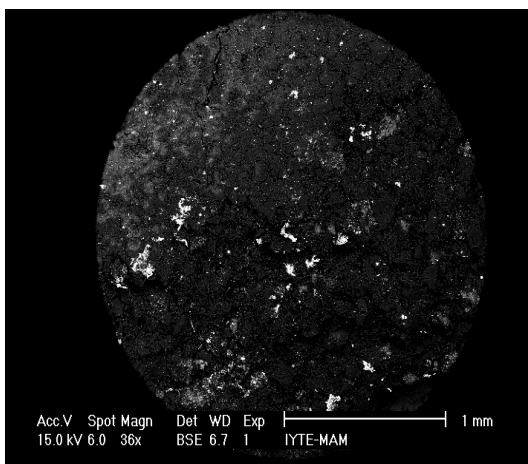
0.01 g Au coated silica



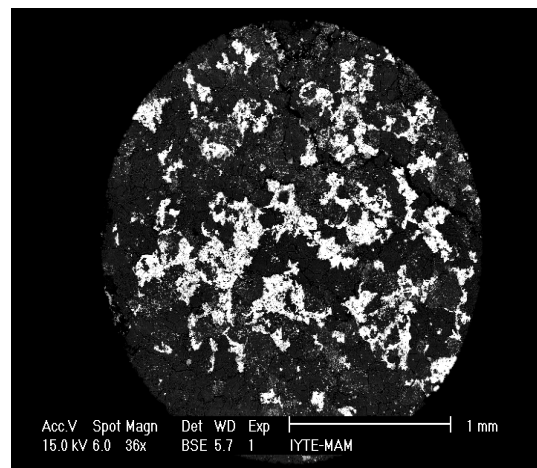
0.05 g Au coated silica



0.1 g Au coated silica



0.25 g Au coated silica



0.5 g Au coated silica

Figure 3.9. SEM back-scattered microimages of silica pellets treated with different concentrations of gold solutions.

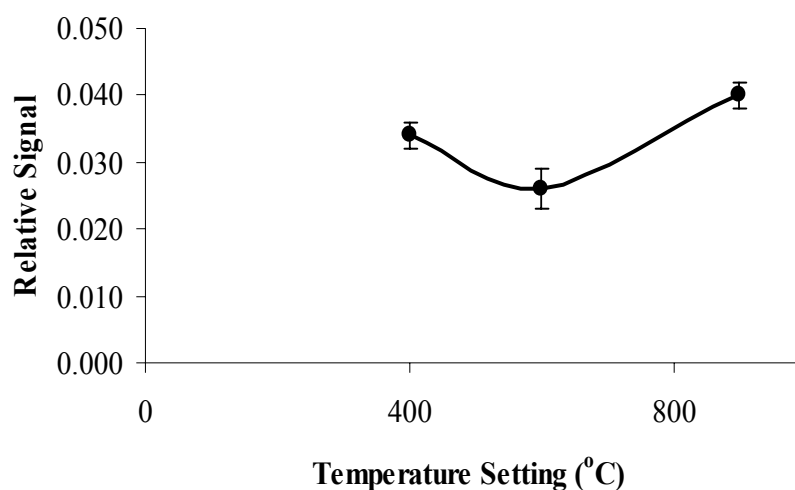


Figure 3.10. Effect of releasing temperature on Hg signal (0.5 g Au-coated silica, 0.7 M HNO₃, 5% (m/v) SnCl₂).

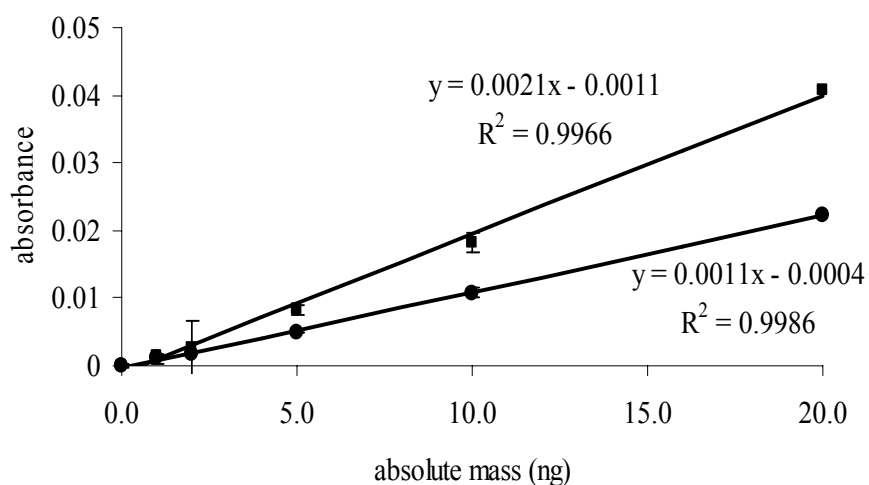
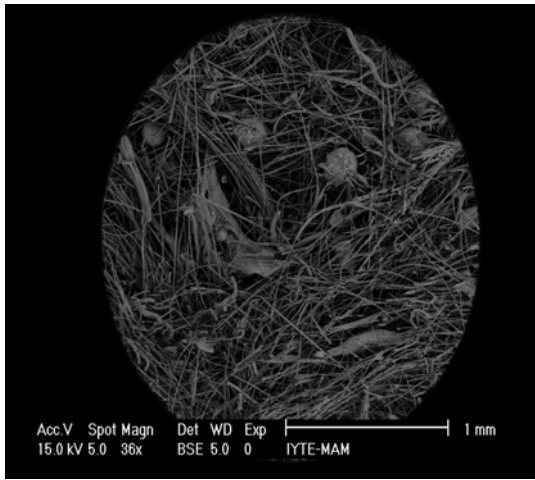


Figure 3.11. Calibration plot with and without amalgamation for silica. (●) without amalgamation, (■) with amalgamation (0.7 M HNO₃, 5% (m/v) SnCl₂, 2.5 ml sample volume).

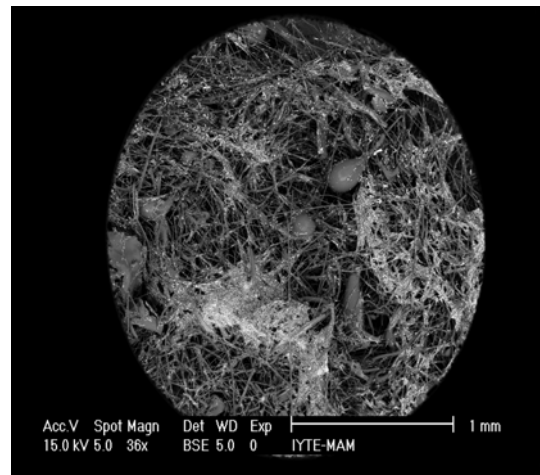
3.4.3. Gold-Coated Quartz Wool

3.4.3.1. Trapping/Releasing Temperature

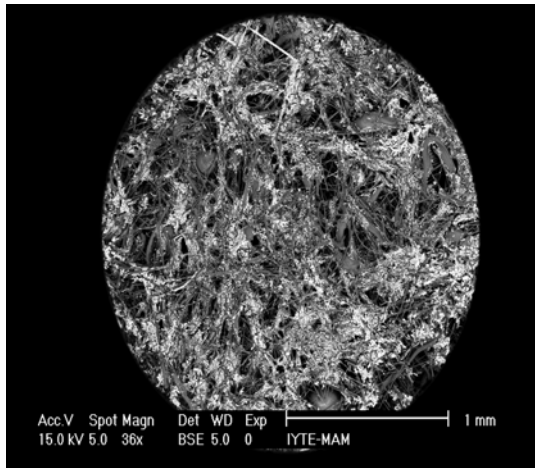
As explained in section 2.6.2, quartz wool was treated with different concentrations of gold solutions (0.1 – 0.5% m/v) and the resultant mixture was cured at 560 °C as in the cases of alumina and silica. The SEM microimages of the surfaces are shown in Figure 3.12. As seen from the figure, all of the coated quartz wool samples show an appreciable gold coating on the surface. Especially, 0.25 g and 0.5 g Au-coated quartz wool samples indicated similar (and relatively homogeneous) covering. However, 0.5 g Au-coated quartz wool was used in the remaining experiments as this material demonstrated the most efficient behavior in terms of mercury trapping. (Although not shown here, EDX results confirmed the same observation; the amount of Au coated on the surface was higher when 0.5 g Au was used in coating step.) It was observed that the trapping of mercury on the Au-coated quartz wool was very efficient, as in the cases of alumina and silica coated with Au, at room temperature. A very important advantage over the other materials, on the other hand, is the ease of operation that can be obtained with quartz wool. The change in Hg signal as a function of temperature setting is shown in Figure 3.13. It can be said that even a temperature of 50 °C can desorb most of the Hg from the amalgamation column; but a temperature setting of 400 °C was applied as a releasing temperature for quartz wool (The actual temperature in the amalgamation column increased up to 500 °C transiently.) The reproducibility of the results was so good that the error bars of the individual results in the graph are very difficult to figure out. In addition, no memory effect was observed as all the sorbed Hg was quickly released from the column.



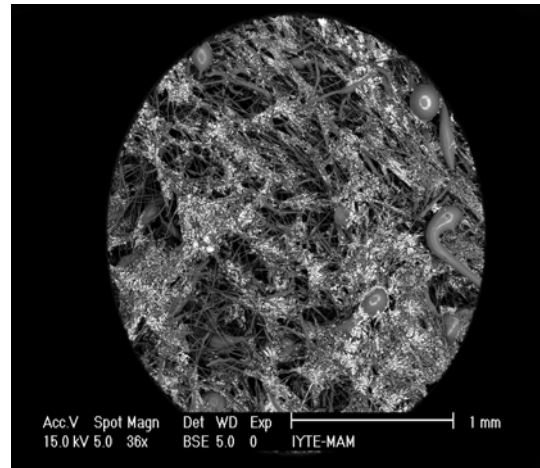
Quartz wool blank



0.1 g Au coated quartz wool



0.25 g Au coated quartz wool



0.5 g Au coated quartz wool

Figure 3.12. SEM back-scattered microimages of quartz wool treated with different concentrations of gold solutions.

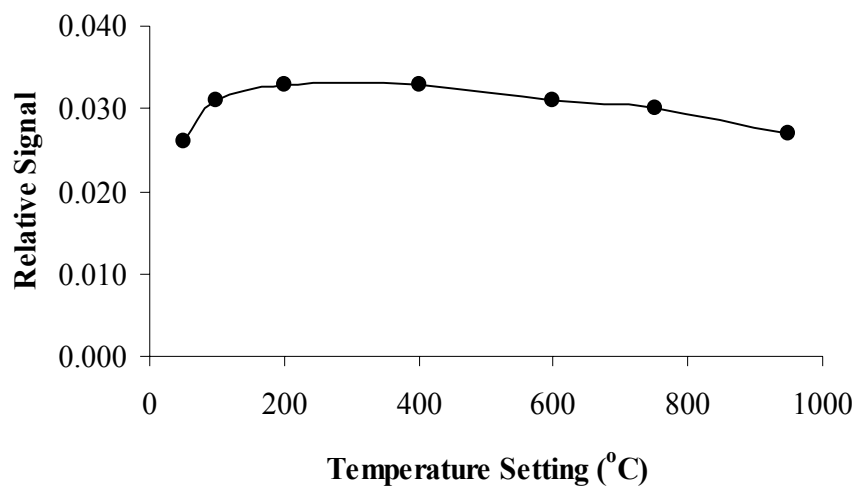


Figure 3.13. Effect of releasing temperature on Hg signal (Au-coated quartz wool, 0.7 M HNO₃, 5% (m/v) SnCl₂).

3.4.3.2. Calibration Plot for Au-Coated Quartz Wool

The calibration graphs of Hg(II) with and without amalgamation with Au-coated quartz wool are shown in Figure 3.14. As obtained previously with the other amalgamation materials, the calibration sensitivity was higher with amalgamation.

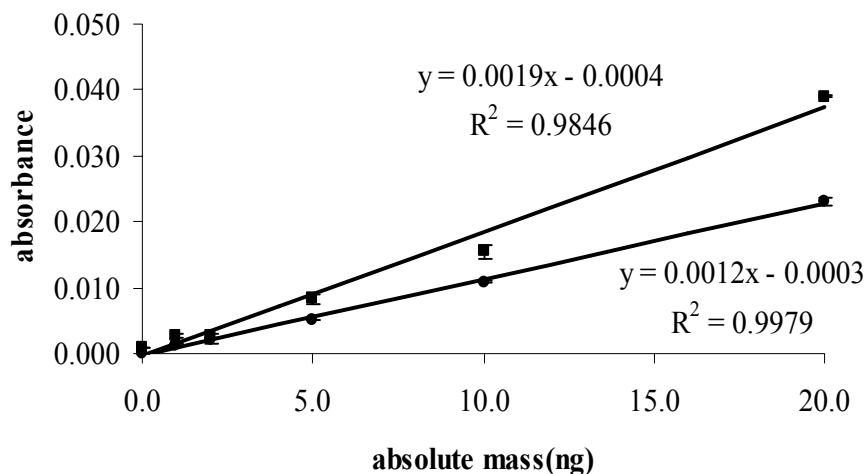


Figure 3.14. Calibration plot with and without amalgamation for quartz wool. (●) without amalgamation, (■) with amalgamation (0.7 M HNO₃, 5% (m/v) SnCl₂, 2.5 ml sample volume).

The enhancement in the calibration sensitivity (slope of the calibration plot) is more pronounced in the case of quartz wool. The signal shapes at the time of measurement (in the “running signal display” mode) can be seen in Figure 3.15. As can be seen from the figure, the actual signal without amalgamation (signal a in the figure) has a larger width at the half maximum whereas it becomes sharper after the amalgamation process (signal b in the figure). The possible reasons for this observation must be, as pointed out in section 3.4.1.1, the release of Hg from a smaller volume and reaching the atomizer without much dilution with the carrier gas. Also, the increase in the rate of Hg released from the column after rapid heating could be the other plausible mechanism. Unfortunately, it was not possible to calculate the peak areas with the current system, but an approximate comparison would indicate that the areas under these two peaks were of similar magnitudes.

The performance of the Au-coated quartz wool was tested with different trapping factors in a way that 20.0 ng Hg was trapped and released using the proposed

methodology. The result of this experiment was considered as the reference value. In the second run, 10.0 ng Hg, was trapped twice in a consecutive manner and the deposited Hg was then released. In the third run, 5.0 ng Hg was trapped four times consecutively and the deposited Hg was released afterwards. The absolute amount of Hg was 20.0 ng in all cases. The results are given in Table 3.3. It can be said that trapping/releasing steps can be acceptable even for a preconcentration factor of four.

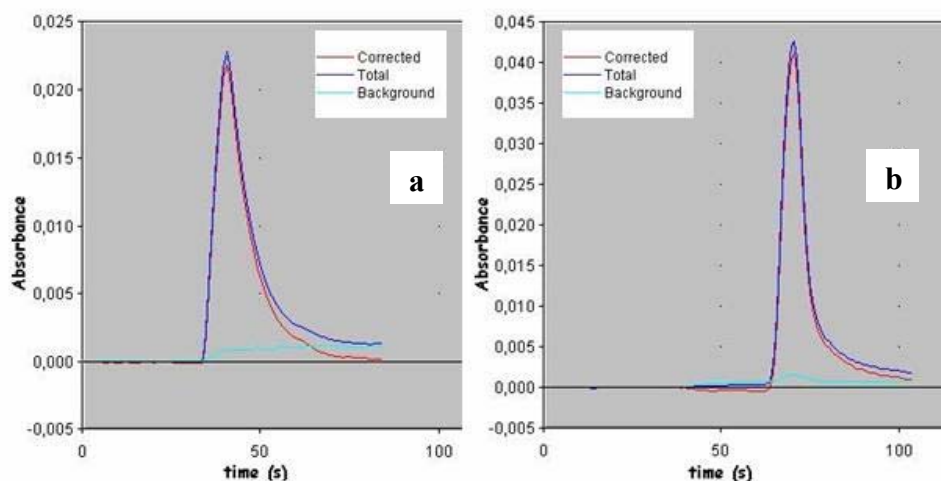


Figure 3.15. Typical transient signals obtained (a) without and (b) with amalgamation step. Note the difference in the magnitude of the y-axes.

Table 3.3. Efficiency of the Au-coated quartz wool in consecutive traps (total amount of Hg was 20.0 ng in all cases).

Initial amount of Hg (ng)	Number of trapping cycles	Recovery (%)
20.0	1	-
10.0	2	102 ± 2
5.0	4	91 ± 5

3.4.4. Gold Sputter-Coated Carbon Fiber

3.4.4.1. Trapping/Releasing Temperature

The sputter-coating process was explained in section 2.4.1.2 and the SEM microimages of the uncoated and coated fibers, as shown in Figure 3.16, demonstrate the efficiency of the sputter-coating process. Gold coating on the surface can easily be seen from the figure on the right whereas no gold is seen on the left (uncoated one). The trapping behavior of the Au sputter-coated carbon fiber was very similar to the other materials tested and was very efficient even at room temperature. In terms of working practice, it was superior to alumina and silica, but inferior to quartz wool. Its releasing behavior was also very similar to quartz wool and a temperature setting of 400 °C was applied at desorption step.

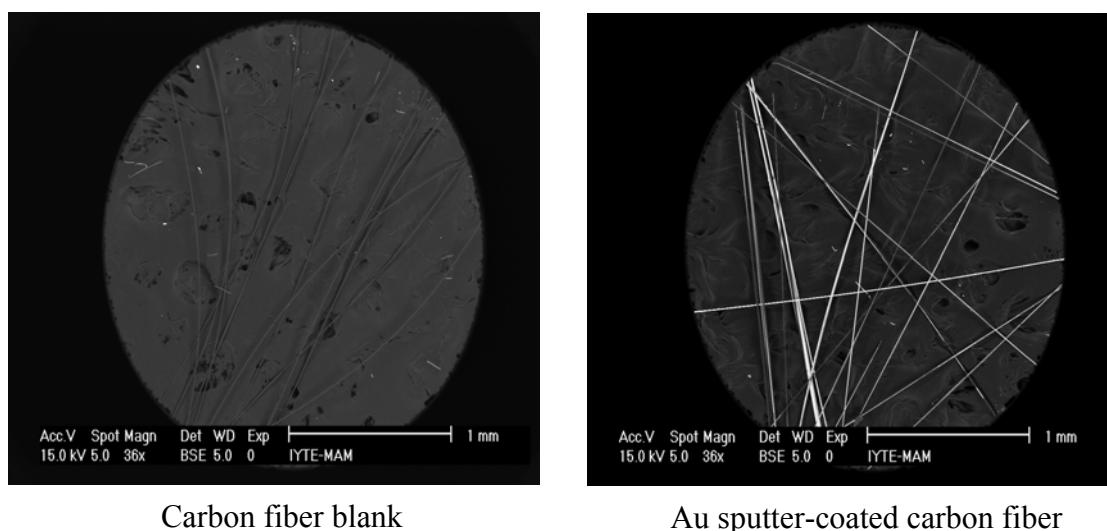


Figure 3.16. SEM back-scattered microimages of carbon fibers sputtered with gold.

3.4.4.2. Calibration Plot for Au Sputter-Coated Carbon Fiber

The calibration graphs of Hg(II) with and without amalgamation with Au sputter-coated carbon fiber are shown in Figure 3.17. As obtained previously with the other materials, the calibration sensitivity was higher with amalgamation. The performance of the Au sputter-coated carbon fiber was tested with different trapping

factors in a similar way to that of quartz wool with the same absolute amounts of Hg. The results, given in Table 3.4, were not as good as those of quartz wool but can be acceptable in many cases.

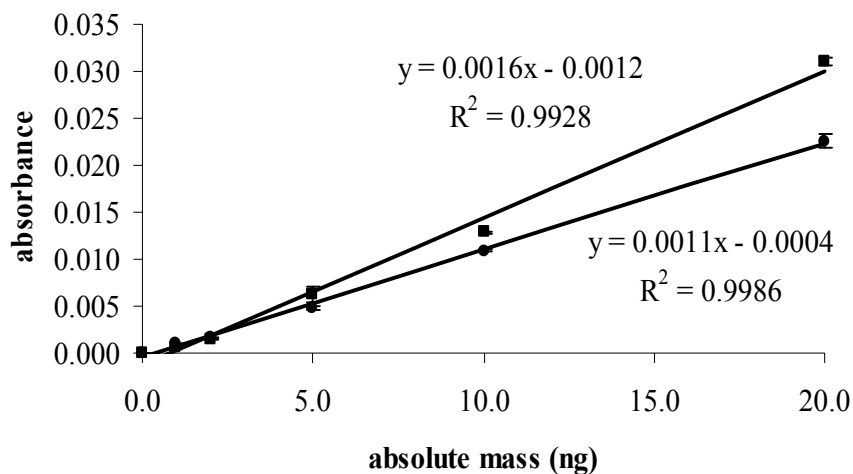


Figure 3.17. Calibration plot with and without amalgamation for carbon fiber. (●) without amalgamation, (■) with amalgamation (0.7 M HNO₃, 5% (m/v) SnCl₂, 2.5 ml sample volume).

Table 3.4. Efficiency of the Au sputter-coated carbon fiber in consecutive traps (total amount of Hg was 20.0 ng in all cases).

Initial amount of Hg (ng)	Number of trapping cycles	Recovery (%)
20.0	1	-
10.0	2	83 ± 10
5.0	4	85 ± 16

From the experiments up to now, it was concluded that the Au-treated quartz wool demonstrated the most promising behavior in Hg amalgamation and therefore the remaining experiments were carried out with this material.

3.5. Analytical Performance of the CVAAS System without and with Amalgamation

3.5.1. Effect of Sample Volume on Calibration Sensitivity

The effect of sample volume on calibration plot (without amalgamation) was investigated using volumes of 2.0, 5.0, and 10.0 ml. For this purpose, various concentrations of Hg(II) solution ($0.1 - 10 \mu\text{g l}^{-1}$) were prepared at the above-mentioned volumes and determined using the optimum conditions. As expected, the mercury signal increases with increasing sample volume (Figure 3.18). It can also be stated that all three volumes can be applied for quantitative determination of Hg in many environmental samples. In terms of repeatability of the results and for the convenience of the reaction in the present 50-ml reaction vessel, 2.0 ml sample volume offers the best results. On the other hand, 5.0 and 10.0 ml sample volumes can be suggested if more sensitive results are required (Hg concentrations below $0.2 \mu\text{g l}^{-1}$ cannot be determined with 2.0 ml sample volume).

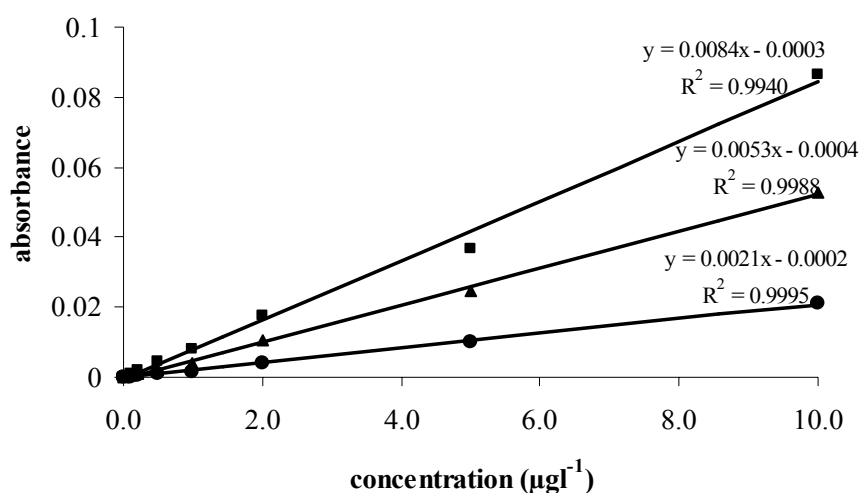


Figure 3.18. Calibration plots for different sample volumes without amalgamation as a function of Hg(II) concentration. (●) 2.0 ml sample volume, (▲) 5.0 ml sample volume, (■) 10 ml sample volume (0.7 M HNO_3 , 5% (m/v) SnCl_2).

When the same points are plotted as a function of absolute mass of Hg (Figure 3.19), it is seen that 2.0 and 5.0 ml gave almost the same absorbance. The slight

loss in sensitivity and repeatability with 10.0 ml sample volume might have been caused by the inefficient mixing of the sample and the reductant in the reaction vessel.

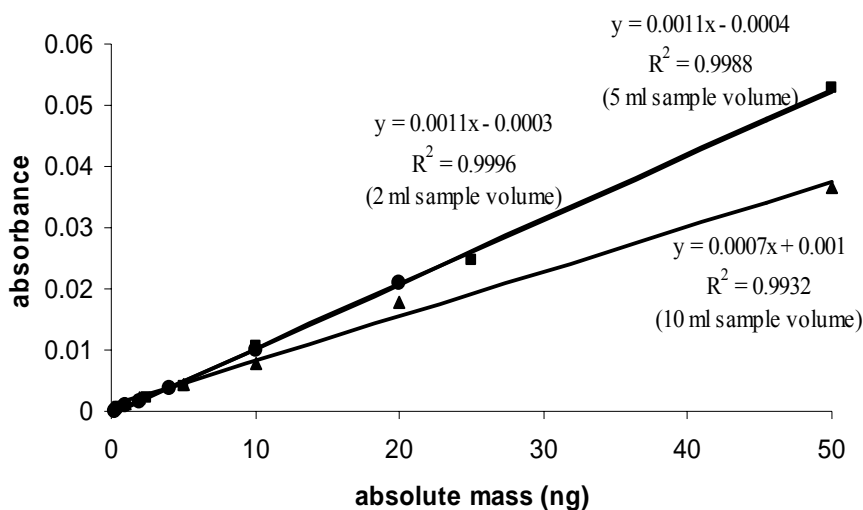


Figure 3.19. Calibration plots for different sample volumes without amalgamation as a function of absolute mass. (●) 2.0 ml sample volume, (■) 5.0 ml sample volume, (▲) 10.0 ml sample volume (0.7 M HNO₃, 5% (m/v) SnCl₂). (Note that 2.0 and 5.0 ml sample volumes gave almost the same calibration plot.)

3.5.2. Effect of Sample Volume on Amalgamation

The advantage of amalgamation in terms of improvement in both the sensitivity and the repeatability can be understood from Figure 3.20. Here, different Hg(II) concentrations and different sample volumes were employed. Hg(II) concentrations and the sample volumes were varied between 0.1 – 5.0 µg l⁻¹ and 2.0 – 10.0 ml, respectively. In Figure 3.20, absorbance was plotted as a function of absolute amount of Hg. It can be concluded that all three volumes can be applied for quantitative determination of Hg after amalgamation due to the similarity of the calibration plots obtained. Within the studied range it can be seen that with amalgamation, the linearity of the calibration plots was not dependant on the sample volume and this property is expected to offer an important advantage since it makes the volume adjustment unnecessary.

The importance of sample volume and amalgamation is more pronounced for low Hg concentrations. The signal shape for 2.0 ml of 0.2 µg l⁻¹ Hg(II) is shown in Figure 3.21. As seen from the figure, 0.2 µg l⁻¹ Hg(II) is almost the limit of

determination with the CVAAS when 2.0 ml sample volume is used (signal a), and lower concentrations cannot be determined. Signal (b) in Figure 3.21 shows the improvement in peak shape and sensitivity when amalgamation is employed.

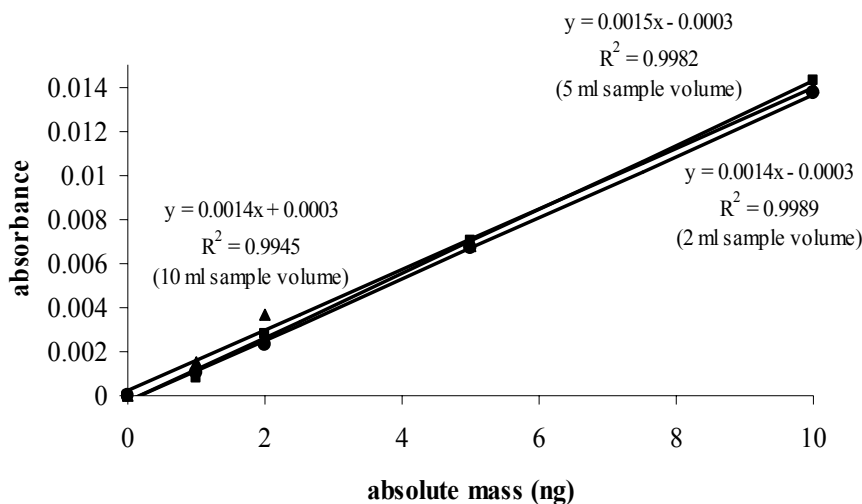


Figure 3.20. Calibration plots for different sample volumes with amalgamation as a function of absolute mass. (●)2.0 ml sample volume, (■) 5.0 ml sample volume, (▲)10.0 ml sample volume, (0.7 M HNO₃, 5% (m/v) SnCl₂).

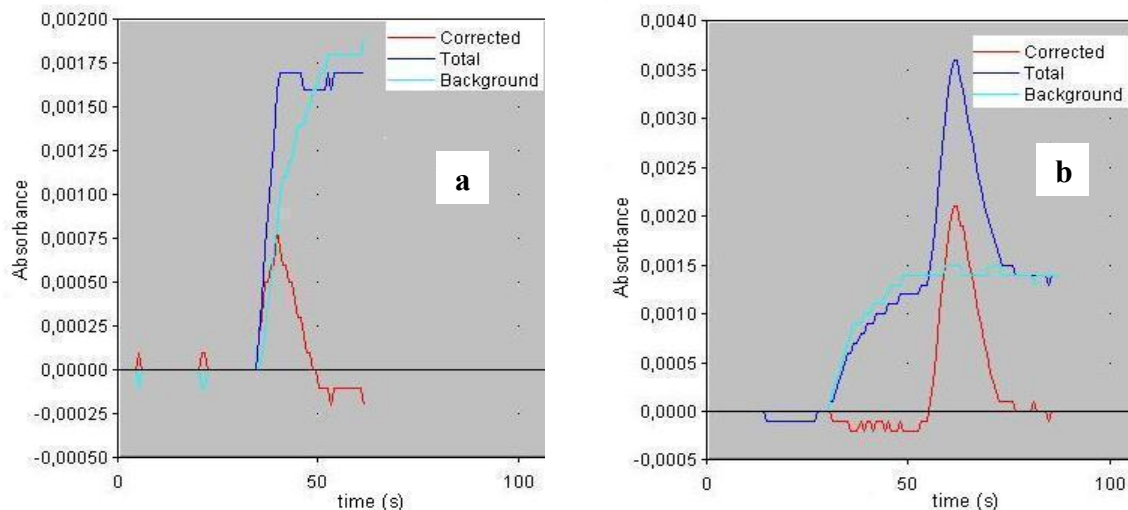


Figure 3.21. Typical transient signals obtained (a) without and (b) with amalgamation step (five times) when 2.0 ml of 0.2 µg l⁻¹ Hg(II) was applied. Note the difference in the magnitude of the y-axes.

When the same procedure was applied with 5.0 ml sample volume having an Hg(II) concentration of 0.1 µg l⁻¹, the signal shapes are as given in Figure 3.22. The improvement in the sensitivity and the signal shape is more easily seen in this figure.

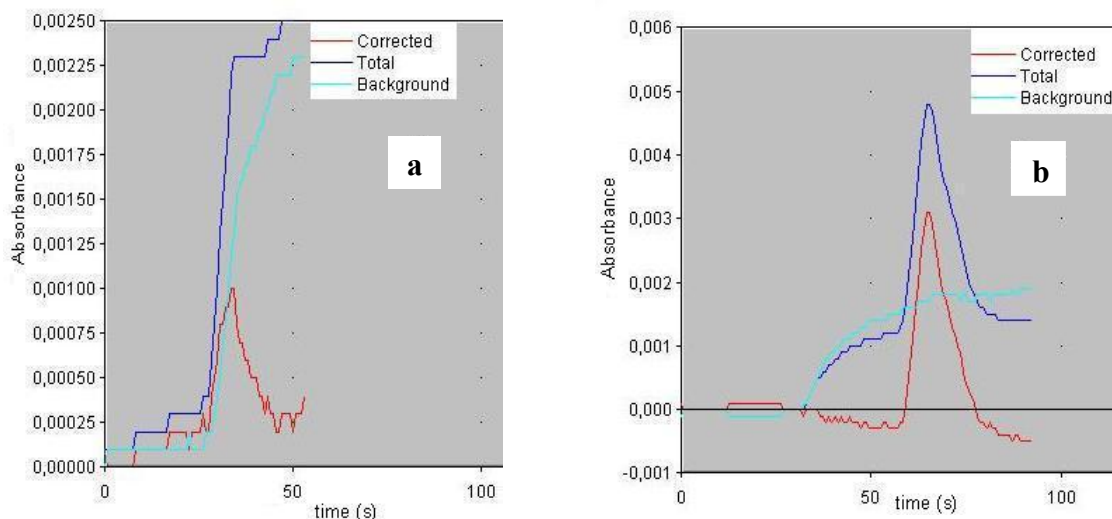


Figure 3.22. Typical transient signals obtained (a) without and (b) with amalgamation step (five times) when 5.0 ml of $0.1 \mu\text{g l}^{-1}$ Hg(II) was applied. Note the difference in the magnitude of the y-axes.

Figure 3.23 demonstrates the CVAAS signals for 10.0 ml of $0.1 \mu\text{g l}^{-1}$ Hg(II), without amalgamation (a), with one-time-trap amalgamation (b) and with five-times-trap amalgamation (c). As it has been mentioned before, the signal shape becomes sharper upon amalgamation even after one-time trapping (signal b). After five consecutive traps with amalgamation system, sensitivity, signal shape and limit of detection are all improved (signal c).

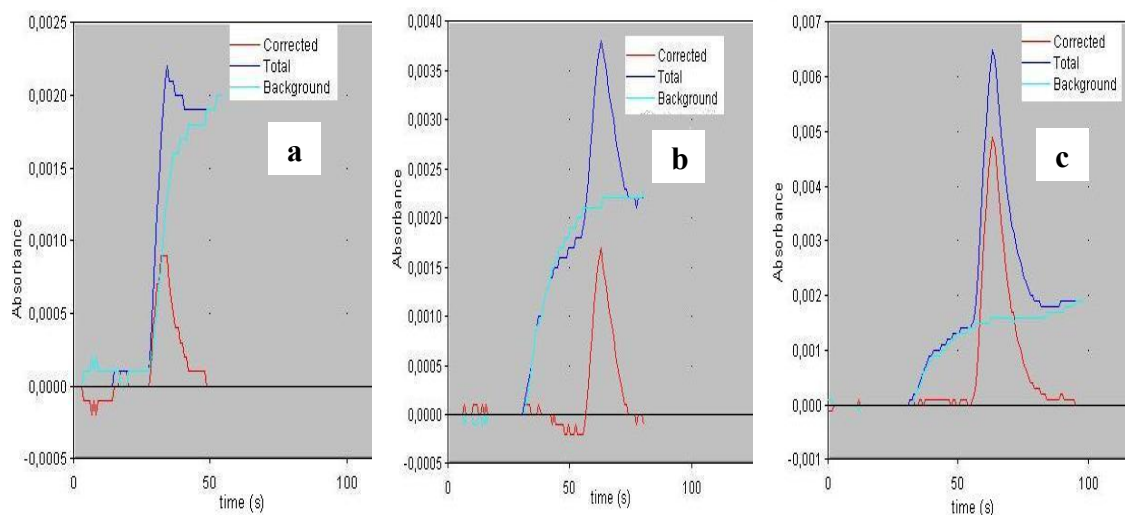


Figure 3.23. Typical transient signals obtained (a) without, (b) trapped once and (c) trapped five times with amalgamation step when 10.0 ml of $0.1 \mu\text{g l}^{-1}$ Hg(II) was applied. Note the difference in the magnitude of the y-axes.

Table 3.5. Limit of detection values for different sample volumes without and with five-times-trap amalgamation (n=3).

volume (ml)	concentration ($\mu\text{g l}^{-1}$)	Limit of detection (3s), $\mu\text{g l}^{-1}$	
		without amalgamation	with amalgamation
2.0	0.2	0.052	0.015
5.0	0.1	0.028	0.019
10.0	0.1	0.027	0.020

The improvement in the limit of detection can also be seen from Table 3.5. Here, standard Hg(II) solutions with the indicated concentrations were prepared and the limit of detection (based on 3s) for each sample volume was calculated before and after amalgamation (5 times trapping). It can be concluded that, amalgamation step improves the limit of detection for each sample volume, with the highest improvement on 2.0 ml.

3.5.3. Application of the Proposed Method to a Real Sample

As demonstrated in sections 3.5.1 and 3.5.2, sample volume is a very important parameter and has a direct influence on the sensitivity of the method. Depending on the concentration of Hg(II) present in the sample, various sample volumes can be employed. In order to investigate the effect of increase in the sample volume of a real water sample (a spring water sample from Karaburun) in the CVAAS system used, it was spiked with $1.0 \mu\text{g l}^{-1}$ Hg(II) and the proposed methodology without and with amalgamation was employed. A similar experiment was repeated with deionized water for comparison. The sample volumes were 1.0, 5.0 and 10.0 ml. As expected, the signal increases with increasing sample volume (Figure 3.24). Here, the important point is that the deionized water and the spring water gave very similar calibration sensitivities at all volumes both without and with amalgamation. These results demonstrate the applicability of the Au-coated quartz wool with amalgamation method to the samples with low Hg concentrations.

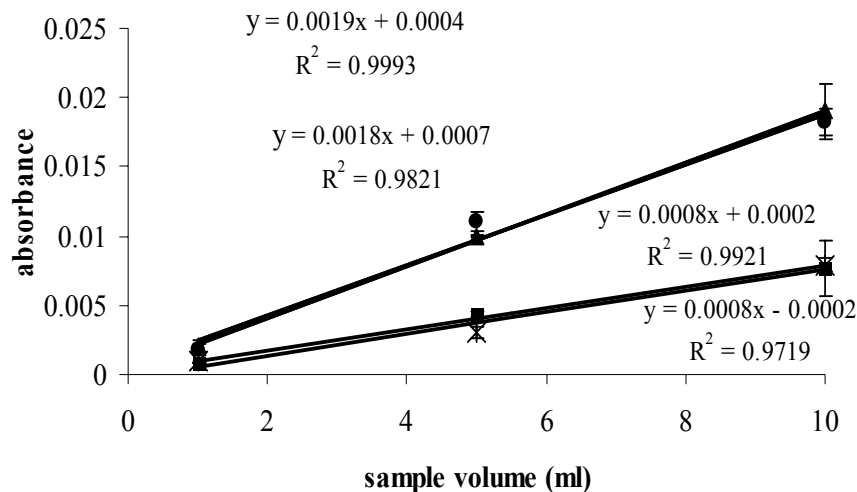


Figure 3.24. The effect of sample volume on trapping/releasing efficiency with and without amalgamation for gold-coated quartz wool. (■) spring water without amalgamation ($y = 0.0008x + 0.0002$, $R^2 = 0.9921$), (●) spring water with amalgamation ($y = 0.0019x + 0.0004$, $R^2 = 0.9993$), (*) deionized water without amalgamation ($y = 0.0008x - 0.0002$, $R^2 = 0.9719$), (▲) deionized water with amalgamation ($y = 0.0018x + 0.0007$, $R^2 = 0.9821$), (0.7 M HNO_3 , 5% (m/v) SnCl_2).

CHAPTER 4

CONCLUSIONS

The initial parts of the present study focused on the optimization of CVAAS parameters; for this purpose, effect of concentration and volume of reductant (SnCl_2), carrier gas flow rate and stirring time were optimized. It was found that 500 μl of 5% (m/v) SnCl_2 was optimum for a sample volume of 2.5 ml. The carrier gas flow rate and stirring time were 700 ml min^{-1} and 60 seconds, respectively.

The second part concentrated on the search for an appropriate sorbent for the separation/enrichment of Hg(II) from waters. It was found that various sorbents could be used for this purpose, but the use of Duolite GT-73, a macroporous resin with thiol (-SH) functional groups, was suggested for better performance. No interference was expected from the other possible species that the resin takes up (e.g. Sb(III) and As(III)), since Hg vapor is generated/separated from the solution by the addition of SnCl_2 and is trapped by a Au-coated amalgamation material.

An amalgamation unit utilizing various Au-coated sorbents was constructed and employed in the determinations. The unit was a combination of IR lamps and coiled Ni-Cr wire for electrical heating which enabled an efficient system. The quartz column filled with the amalgamation material was incorporated into the spiral Ni-Cr wire.

The performance of four different Au-coated amalgamation materials was examined throughout the study; alumina, silica, quartz wool and carbon fibers. All of the materials have been shown to be applicable for Hg amalgamation, but quartz wool and carbon fibers were found to be the most efficient.

Analytical performance of the CVAAS system in terms of sample volume, limit of detection, and without/with amalgamation was investigated in the last part of the study. Gold-coated quartz wool was employed in the amalgamation column. It was observed that the mercury signal increased with increasing sample volume, as expected. On the other hand, provided that the absolute amount of Hg(II) was kept constant while changing the sample volume, use of amalgamation unit resulted in similar calibration sensitivities. With amalgamation, the linearity and the slope of the calibration plots were not dependant on the sample volume and this property is expected to offer an important advantage since it makes the volume adjustment unnecessary.

The limit of detection was also improved with amalgamation. The highest improvement was obtained with 2.0 ml sample volume; the limit of detection was 3.5 times lower (3.5 times better) than that of without amalgamation when 5-times trapping was employed.

Finally, the analytical performance of the proposed method was tested on a real sample, spring water taken from Karaburun. The results demonstrated that the methodology can be applied to these types of samples directly or after amalgamation, depending on Hg(II) concentration.

REFERENCES

- Abbas, M.N. and Mostafa, G.A.E. 2002. "New Triiodomercurate-Modified Carbon Paste Electrode for the Potentiometric Determination of Mercury," *Analytica Chimica Acta*. Vol. 478, p. 329.
- Andac, M., Asan, A., Bekdemir, Y., Kutuk, H. and Isildak, I. 2003. "Spectrophotometric Flow-Injection Analysis of Mercury(II) in Pharmaceuticals with P-Nitrobenzoxosulfamate," *Talanta*. Vol. 60, p. 191.
- Anderson, K.A., 2000. *Mercury Analysis in Environmental Samples by Cold Vapor Techniques in Encyclopedia of Analytical Chemistry: Instrumentation and Applications*, (John Wiley and Sons, Chichester), p. 2894, 2905-2906, 2910.
- Bagheri, H. and Gholami, A. 2001. "Determination of Very Low Levels of Dissolved Mercury(II) and Methyl Mercury in River Waters by Continuous Flow with On-line UV Decomposition and Cold Vapor Atomic Fluorescence Spectrometry after Preconcentration on a Silica Gel-2-Mercaptobenzimidazol Sorbent," *Talanta*. Vol. 55, p. 1141.
- Bennun, L., Gillette, V.H. and Greaves, E.D. 1999. "Data Processing Technique for Mercury Determination by Total-Reflection X-Ray Fluorescence, Using Amalgamation with Gold" *Spectrochimica Acta Part B*. Vol. 54, p. 1291.
- Bouyssiere, B., Baco, F., Savary, L. and Lobinski, R. 2002. "Speciation Analysis of Mercury in Gas Condensates by Capillary Gas Chromatography with Inductively Coupled Plasma Mass Spectrometric Detection," *Journal of Chromatography A*. Vol. 976, p. 431.
- Camel, V. 2003. "Solid Phase Extraction of Trace Elements," *Spectrochimica Acta part B*. Vol. 58, p. 1177.
- Costley, C.T., Mossop, K.F., Dean, J.R., Garden, L.M., Marshall, J. and Carroll, J. 2000. "Determination of Mercury In Environmental and Biological Samples Using Pyrolysis Atomic Absorption Spectrometry with Gold Amalgamation," *Analytica Chimica Acta*. Vol. 405, p. 179.
- Council of the European Union. "Council Directive 98/83/EC of 3 November 1998 on the quality of water intended for human consumption," *Official Journal L*, 330, (1998), 32.
- Dietz, C., Madrid, Y. and Camara, C. 2001. "Mercury Speciation Using the Capillary Cold Trap with Microwave-Induced Plasma Atomic Emission Spectroscopy," *Journal of Analytical Atomic Spectrometry*. Vol. 16, p. 1397.
- Ebdon, L., Evans, E.H., Fisher, A. and Hill, S.J., 1998. *An Introduction to Analytical Atomic Spectrometry*, (John Wiley and Sons, Chichester), p. 151-152.

- Fifield, F.W. and Haines, P.J. 1995. *Environmental Analytical Chemistry*, (Chapman and Hall, London), p. 280-290, 320-351.
- Gracia, L.G. and Castro, M.D.L. 1999. "Determination of Mercury in Cosmetics by Flow Injection-Cold Vapor Generation-Atomic Fluorescence Spectrometry with On-Line Preconcentration," *Journal of Analytical Atomic Spectrometry*. Vol. 14, p. 1615.
- Guo, Y. and Guadalupe, A.R. 1999. "Preconcentration and Voltammetry of Mercury on a Functionalized Sol-Gel Thin Film Modified Glassy Carbon Electrode," *Journal of Pharmaceutical and Biomedical Analysis*. Vol. 19, p. 175.
- Haswell, S.J., 1999. *Atomic Absorption Spectrometry Theory Design and Applications-Volume 5*, (John Wiley), p. 34.
- Hinds, M.W. 1998. "Determination of Mercury in Gold Bullion by Flame and Graphite Furnace Atomic Absorption Spectrometry," *Spectrochimica Acta B*. Vol. 53, p. 1063.
- Howard, A.G., 1997. *Aquatic Environmental Chemistry*, (Oxford Science Publications, Southampton), p. 35.
- Keating, M.H., Mahaffey, K.R., Schoeny, R., Rice, G.E., Bullock, O.R., Ambrose, R.B., Swartout, J. and Nichols, J.W. 1997. "Mercury Study Report to Congress-Volume I: Executive Summary", Office of Air Quality Planning and Standards and Office of Research Development, (December 1997), U.S. Environmental Protection Agency, Vol. 1, p.1-95.
- Kopysc, E., Pryzyska, K., Garbos, S. and Bulska, E. 2000. "Determination of Mercury by Cold-Vapor Atomic Absorption Spectrometry with Preconcentration on a Gold-Trap," *Analytical Sciences*. Vol. 16, p.1309.
- Lawes, G., 1998. *SEM Instrumentation in Scanning Electron Microscopy and X-Ray Microanalysis*, (John Wiley&Sons, London), pp. 1-20, 78-79. [p.3, 6, 11]
- Li, Y., Jiang, Y., Yan, X.P. and Ni, Z.M. 2002. "Determination of Trace Mercury in Environmental and Foods Samples by Online Coupling of Flow Injection Displacement Sorption Preconcentration to Electrothermal Atomic Absorption Spectrometry," *Environmental Science and Technology*. Vol.36, p. 4886.
- Magalhaes, C.E.C., Krug, F.J., Fostier, A.H. and Berndt, H. 1997. "Direct Determination of Mercury in Sediments by Atomic Absorption Spectrometry," *Journal of Analytical Atomic Spectrometry*. Vol. 12, p. 1231.
- Mester, Z., Lam, J., Sturgeon, R. and Pawliszyn, J. 2000. "Determination of Methylmercury by Solid-Phase Microextraction Inductively Coupled Plasma Mass Spectrometry: A New Sample Introduction Method for Volatile Metal Species," *Journal of Analytical Atomic Spectrometry*. Vol. 2000, p.837.

- Mondal, B.C. and Das, A.K. 2003. "Determination of Mercury Species with a Resin Functionalized with A 1,2-Bis(O-Aminophenylthio)Ethane Moiety," *Analytica Chimica Acta*. Vol. 477, p. 73.
- Monteiro, A. C. P. M., Andrade, L. S. N., Luna, A. S., Campos, R. C. 2002. "Sequential Quantification of Methyl Mercury in Biological Materials by Selective Reduction in The Presence of Mercury(II), Using Two Gas-Liquid Separators," *Spectrochimica Acta part B*. Vol. 57, p. 2103.
- Nakagawa, R. 1999. "Estimation of Mercury Emissions from Geothermal Activity in Japan," *Chemosphere*. Vol. 38, p. 1867.
- Neto, J.A.G., Zara, L.F., Rocha, J.C., Santos, A., Dakuzaku, C.S. and Nobrega, J.A. 2000. "Determination of Mercury in Agroindustrial Samples by Flow-Injection Cold Vapor Atomic Absorption Spectrometry Using Ion Exchange and Reductive Elution," *Talanta*. Vol. 51, p. 587.
- O'Connor, D.J. and Sexton, B.A. 1992. *Electron Microscope Techniques for Surface Characterization in Surface Analysis Methods in Materials Science*, (Springer, Berlin), pp. 13-15, 87-99.
- Pager, Cs. and Gaspar, A. 2002. "Possibilities of Determination of Mercury Compounds Using Capillary Zone Electrophoresis," *Microchemical Journal*. Vol. 73, p. 53.
- Pineiro, J.M., Mahia, P.L., Lorenzo, S.M., Fernandez, E.F. and Rodriguez, D.P. 2002. "Direct Mercury Determination in Aqueous Slurries of Environmental and Biological Samples by Cold Vapor Electrothermal Atomic Absorption Spectrometry," *Analytica Chimica Acta*. Vol. 460, p. 111.
- Sandor, M., Geistmann, F. and Schuster, M. 1999. "An Anthracene-Substituted Benzoylthiourea for the Selective Determination of Hg(II) in Micellar Media," *Analytica Chimica Acta*. Vol. 388, p.19.
- Skoog, D.A. and West, D.M., 1971. *Principles of Instrumental Analysis*, (Hardcover, New York, USA), p.549.
- Sun, Y.C., Mierzwa, J., Chung, Y.T. and Yang, M.H. 1997. "Differentiation of Mercury and Methylmercury by Direct in-situ Derivatization and Supercritical Fluid Extraction," *Analytical Communications*. Vol. 34, p. 333.
- Tanida, K. and Hoshino M. 1990. "Continuous Determination of Mercury in Air by Gold Amalgamation and Flameless Atomic Absorption," *The Rigaku Journal*. Vol. 7, p. 35.
- Truitt, R.E. and Weber, J.H. 1979. "Trace Metal Ion Filtration at pH 5 and 7," *Analytical Chemistry*. Vol. 51, p. 2057.
- WEB_1, 2004. Web Elements, 10/04/2004. <http://www.webelements.com>

- WEB_2, 2005. Environmental Protection Agency (EPA), 12/04/2005.
<http://www.epa.gov.tr>
- Welz, B. 1998. "Speciation Analysis: The Future of Atomic Absorption Spectrometry," *Journal of Analytical Atomic Spectrometry*. Vol. 13, p. 413.
- Welz, B. and Sperling, M. 1999. *Atomic Absorption Spectrometry*, (WILEY-VCH, Weinheim), p. 47-48, 222-223, 523-524.
- Wuilloud, J.C.A., Willoud, R.G., Olsina, R.A. and Martinez, L.D. 2002. "Separation and Preconcentration of Inorganic and Organomercury Species in Water Samples Using A Selective Reagent and an Anion Exchange Resin and Determination by Flow Injection-Cold Vapor Atomic Absorption Spectrometry," *Journal of Analytical Atomic Spectrometry*. Vol. 17, p. 389.
- Wuilloud, J.C.A., Wuilloud, R.G., Silva, M.F., Olsina, R.A. and Martinez, L.D. 2002b. "Sensitive Determination of Mercury in Tap Water by Cloud Point Extraction Preconcentration and Flow Injection-Cold Vapor-Inductively Coupled Plasma Optical Emission Spectrometry," *Spectrochimica Acta Part B*. Vol. 57, p. 365.
- Wurl, O., Elsholz, O. and Ebinghaus, R. 2000. "Flow System Device for the On-Line Determination of Total Mercury in Sea Water," *Talanta*. Vol. 52, p.51.
- Yang, L., Zhang, D. and Zhou, Q. 2002. "Determination of Mercury in Biological Tissues by Graphite-Furnace Atomic Absorption Spectrometry with an *In-Situ* Concentration Technique," *Analytical Sciences*. Vol. 18, p. 811.
- Zachariadis, G.A., Anthemidis, A.N., Karpouzi, M. and Stratis, J.A. 2003. "On-Line Preconcentration of Mercury Using an Integrated Column/Gas-Liquid Separator (PCGLS) and Cold Vapor Atomic Absorption Spectrometry," *Journal of Analytical Atomic Spectrometry*. Vol. 18, p. 1274.